# 6

# The Human Eye and Adaptive Optics

Fuensanta A. Vera-Díaz and Nathan Doble
*The New England College of Optometry, Boston MA, USA*

## 1. Introduction

Scientists have rapidly taken advantage of adaptive optics (AO) technology for the study of the human visual system. Vision, the primary human sense, begins with light entering the eye and the formation of an image on the retina (Fig 1), where light is transformed into electro-chemical impulses that travel towards the brain. The eye provides the only direct view of the central nervous system and is, therefore, the subject of intense interest as a means for the early detection of a host of retinal and possibly systemic diseases. However, ocular aberrations limit the optical quality of the human eye, thus reducing image contrast and resolution. With the use of AO it is now routinely possible to compensate for these ocular aberrations and image cellular level structures such as retinal cone and rod photoreceptors (Liang et al, 1997; Doble et al, 2011), the smaller foveal cones (Putnam et al, 2010), retinal pigment epithelium (RPE) cells (Roorda et al, 2007), leukocyte blood cells (Martin & Roorda, 2005) and the smallest retinal blood vessels (Tam et al, 2010; Wang et al, 2011), *in vivo* and without the aid of contrast enhancing agents.

The chapter begins with a review of the structure of the human eye before describing the challenges and approaches in using AO to study the visual system.

### 1.1 The human eye and visual system

The human eye behaves as a complex optical structure sensitive to wavelengths between 380 and 760 nm. Light entering the eye is refracted as it passes from air through the tear film-cornea interface. It then travels through the aqueous humor and the pupil (a diaphragm controlled by the iris) and is further refracted by the crystalline lens before passing through the vitreous humor and impinging on the retina (Fig 1). The tear film-cornea interface and the crystalline lens are the major refractive components in the eye and act together as a compound lens to project an inverted image onto the light sensitive retina. From the retina, the electrical signals are transmitted to the visual cortex via the optic nerve (Fig 1). A summary of this path is presented in this section, for detailed information on the anatomy and physiology of the eye the reader is directed to the references (Snell & Lemp, 1998; Kaufman & Alm, 2002; Netter, 2006).

#### 1.1.1 Tear film-cornea interface

The tear film–cornea interface (Fig 1) is the most anterior refractive surface of the eye as well as the most powerful due to the difference between its refractive index and that of air. The

anterior radius of the tear film-cornea interface is approximately 7.80 mm and the refractive index of the tear film is 1.336, which give a dioptric power of approximately 43.00 diopters. Therefore, small variations in its curvature can cause significant changes in the power of the eye.

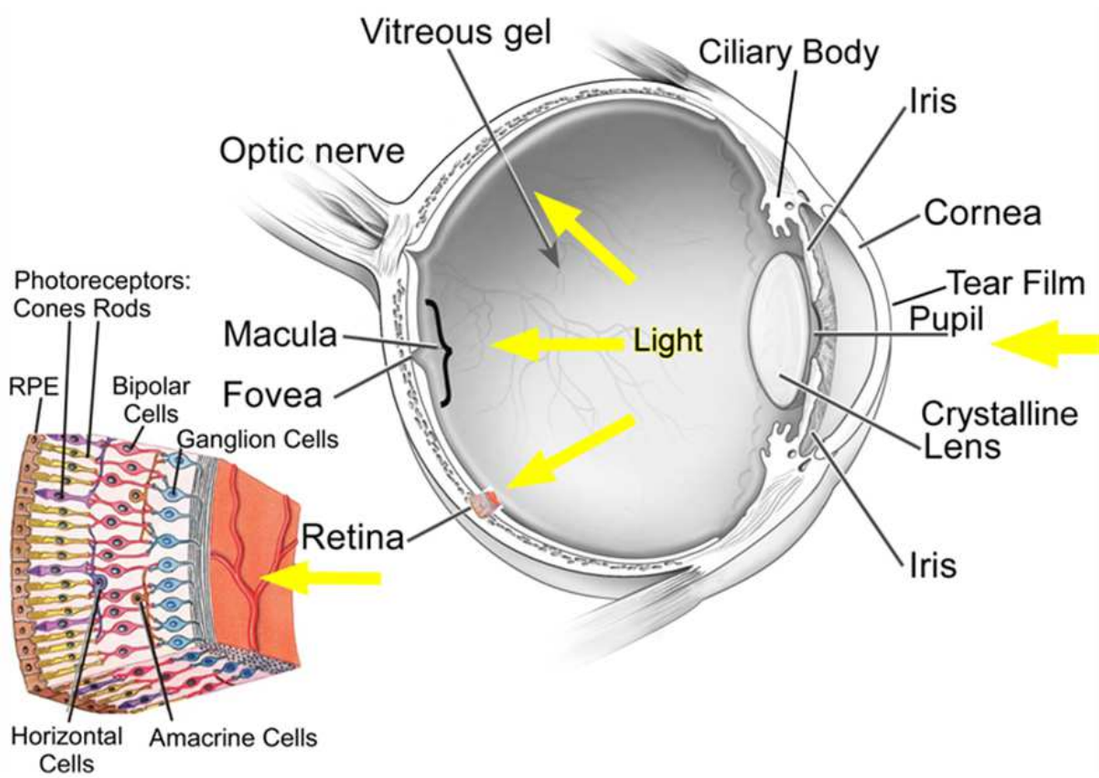


Fig. 1. Gross anatomy of the human eye and detail of the retina.
The major refractive elements and hence primary sources of aberration are the tear film–cornea interface and the crystalline lens. The incident light on the retina is absorbed by the cone and rod photoreceptors after traversing several retinal layers. Image modified from the National Eye Institute, National Institutes of Health.

The cornea is a transparent tissue, achieved by its regular composition of collagen fibers, avascularity and an effective endothelial pump. The cornea in the adult typically measures 10.5 mm vertically and 11.5 mm horizontally and its thickness increases from the center (about 530 μm) to the periphery (about 650 μm). The cornea is more curved than the eyeball and hence protrudes anteriorly. Behind the cornea, the aqueous humor has the same refractive index as the vitreous humor (1.336), whereas the refractive index of the cornea is 1.376. Because the change in refractive index between cornea and aqueous humor is relatively small compared to the change at the air–cornea interface, it has a negligible refractive effect.

### 1.1.2 Crystalline lens. Accommodation

The crystalline lens is held behind the iris by thin yet strong ligaments, zonules of Zinn, attached to the ciliary processes in the ciliary body (Fig 1). The crystalline lens is flexible and

may change its shape using the mechanism of accommodation, by adjusting the ciliary muscle so that the images may be more accurately focused on the retina. It has an ellipsoidal, biconvex shape with the posterior surface being more curved than the anterior. The crystalline lens is typically 10 mm in diameter and has a thickness of approximately 4mm, although its size and shape changes during accommodation, and it continues to grow throughout a person's lifetime. The crystalline lens achieves transparency due to its composition, as 90 % of it is formed by tightly packed proteins and there is an absence of organelles such as a nucleus, endoplasmic reticulum and mitochondria within the mature lens fibers.

The intensity of the light reaching the retina is regulated by the diaphragm formed by the iris: the pupil. The pupil is therefore important in regulating the aberrations of the eye, the magnitude of the aberrations increase with larger pupil diameters – section 1.2.1.

### 1.1.3 Retina

Upon reaching the retinal surface, the light traverses its many layers (Fig 1) before reaching the photoreceptor cells, where the photons are absorbed and transformed into electro-chemical impulses. The gross anatomy of the retina is composed of a macula or central region, with the fovea as the very center. At the fovea the cone photoreceptors have the smallest diameter (1.9-3.4 μm), the highest average density (199,000 cones per $mm^2$) (Curcio & Allen, 1990) and the eye has the highest resolution (visual acuity, VA). The signals from these photoreceptors are then processed by the many intervening cell types in the retina before exiting towards the brain via the ganglion cells and the optic nerve.

i. Physiology of the Photoreceptors: Rods and Cones

The photoreceptors are photosensitive cells located in the outermost layer of the retina that are responsible for the phototransduction, i.e. they convert photons into electro-chemical signals that can stimulate biological processes. The proteins (opsins) in the outer segments of these photoreceptors absorb photons and trigger a cascade of changes in the membrane potential; this mechanism is called the signal transduction pathway. In brief, the photoreceptors signal their absorption of photons via a decrease in the release of the neurotransmitter glutamate to the bipolar cells. The photoreceptors are depolarized in the dark, when a high amount of glutamate is being released, and after absorption of a photon they hyperpolarize so less glutamate is released to the presynaptic terminal of the bipolar cells.

The effect of glutamate in the bipolar cells varies depending on the type of receptor imbedded in the bipolar cell's membrane; it may depolarize or hyperpolarize the bipolar cell. This allows one population of bipolar cells to get excited by light whereas another population is inhibited by it, even though all photoreceptors show the same response to light. This complexity is necessary for various visual functions such as detection of colour, contrast or edges. The complexity increases as there are interconnections among bipolar cells, horizontal cells and amacrine cells in the retina. The final result of this complex net is several populations of different classes of ganglion cells that have specific functions in the retina and exit the eye through the optic nerve.

The photoreceptor cells are the rods and cones (Fig 1, 2), named as consequence of their anatomy. Rods are narrower and distributed mostly in the peripheral retina. A third class

of light cells are the photosensitive ganglion cells, discovered in the 1990s (for a review see (Do & Yau, 2010)), which use the photopigment melanopsin and are believed to support circadian rhythm but do not contribute significantly to vision. The human retina contains approximately 120 million rods and 5 million cones, although this amount varies with age and certain retinal diseases. There are also major functional differences between the rods and cones. Rods are extremely sensitive, have more pigment and can be triggered by a very small number of photons. Therefore, at very low light levels (scotopic vision), the visual signal is coming solely from rods. Rods are almost absent in the fovea, and only a small amount are present in the macular area. Cones, on the other hand, are only sensitive to direct and large amounts of photons; and are used for photopic vision. In humans there are three different types of cone cells that respond approximately to short (S), medium (M) and long (L) wavelengths.

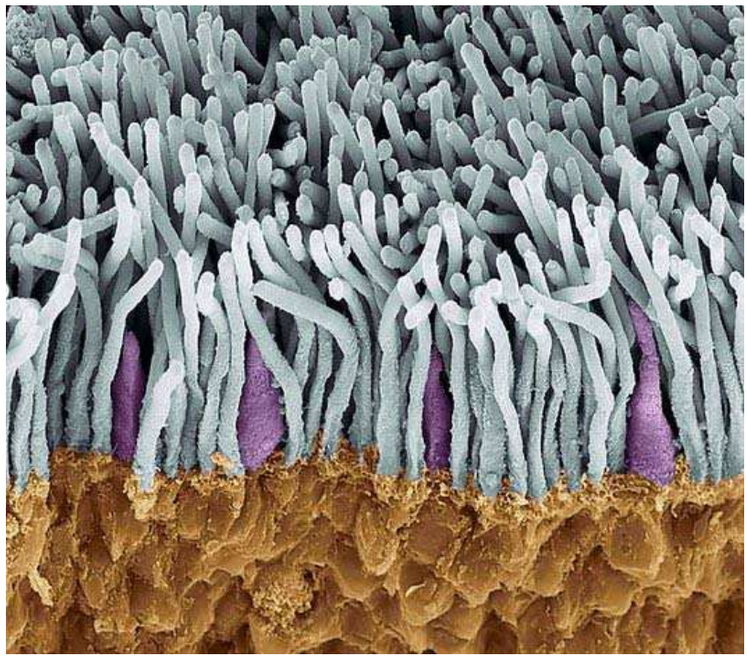

Fig. 2. Colored scanning electron micrograph (SEM) of rods (blue) and cones (purple) in the retina of the eye. The outer nuclear layer is brown. Magnification x1800 when printed at 10 centimetres wide. By Steve Gschmeissner. Reproduced with permission from Science Photo Library.

There is a dependence on photoreceptor arrangement with retinal eccentricity, decreasing in regularity and density from the fovea toward the periphery, although the smallest cones are not always located in the center of the fovea (Chui et al, 2008a). At a given retinal location, there is considerable individual variation in cone photoreceptor packing density, although more than 20 % of the variance could be accounted for by differences in axial length (Chui et al, 2008b).

ii. Waveguide Properties of the Photoreceptors: The Stiles-Crawford Effect

As mentioned above, cones are sensitive to large amounts of light and only if it is directly incident on them. There is, therefore, a reduction in light sensitivity when its entry point is shifted from the center to the edge of the pupil. This phenomenon, called the Stiles-

Crawford Effect (SCE) (Stiles & Crawford, 1933; Westheimer, 2008), plays an important role in vision because unwanted scattered light is rejected. Individual cones have specific waveguiding properties (Enoch, 1963), cone disarray is very small in healthy eyes and ensembles of cones have essentially the same directionality properties as a single cone (Roorda & Williams, 2002). This property of the photoreceptors shows small variations across the retinal field (Westheimer, 1967; Burns et al, 1997). It has been suggested (Vohnsen, 2007) that the photoreceptors may be at least partially adapted to match the average ocular aberrations in order to maximize their light-capturing capabilities.

The study of SCE may provide useful information about subtle structural changes in retinal disease, changes that may not be detected with conventional clinical tests. It has been shown that this property of the photoreceptors is altered in central serous chorioretinopathy (Kanis & van Norren, 2008). Delayed recovery of photoreceptor directionality was found when measuring SCE at a stage of the disease when no abnormalities were found using other common diagnostic techniques such as VA and optical coherence tomography (OCT). Transient changes of the SCE have also been found in the near periphery of myopic eyes with elongated axial lengths (Choi et al, 2004) and in eyes with permanent visual field loss and damage of the inner retinal layers secondary to optic neuropathies (Choi et al, 2008).

iii. Temporal Properties of the Photoreceptors

The photoreceptors outer segments contain discs studded with opsins that capture photons to initiate the phototransduction process. Throughout the day, new discs are added, dozens of discs are shed and phagocytosis occurs at the RPE. *In vivo* detection of disc renewal has only been possible recently with the use of AO. Using an AO flood-illuminated camera, Pallikaris et al (2003) observed changes in cone reflectance over a 24 hour period using non-coherent illumination. These changes were incoherent, not sinusoidal, with both rapid, over minutes, and slow, over hours, changes. They also found these changes to be independent from cone to cone. Hence, they concluded that the changes are not caused by spatiotemporal variation in the optical axes of the cones but were likely caused by changes in the composition of the outer segment-RPE interface due to the migration of melanosomes during disc shedding, or a change in refractive index in the outer segment interface during shedding. If the reflectance changes are related to the renewal process of the receptors, it will be possible to study disruptions in the disc shedding process that occur in diseases such as retinitis pigmentosa.

Other authors have shown faster cone changes. Jonnal et al (2007) showed rapid changes in reflectance in response to visible stimulation of individual photoreceptors. These changes are initiated 5 to 10 msec after the onset of the stimulus flash and last 300 to 400 msec and are believed to be linked to the process of cone phototransduction. Possible mechanisms for this phenomenon are processes taking place within the cone immediately following stimulation, such as changes in the concentration of G-proteins, hyperpolarization or other changes in the properties of the outer segment membrane, or changes in the physical size of the outer segment secondary to swelling.

Jonnal et al (2010) reported the period for cone reflectance oscillation when using long coherent illumination to range between 2.5 and 3 hours, with sinusoidal oscillations occurring during a 24 hour period. The power spectra of most cones peaked at a frequency

between 0.3 and 0.4 cycles/hour, although this peak varied within a 24 hour period. They hypothesized that these oscillations are due to elongation of the cones outer segments (OS) (Jonnal et al, 2010). These rates agree with post-mortem studies in mammals on OS renewal rates on rods (~2μm /day) and cones (~ 1-3μm/day).

### 1.1.4 The visual system

In brief, the electrical signals at the retina exit each eye via ganglion cells axons through the optic nerve, following a path that crosses at the optic chiasma to later reach the lateral geniculate nucleus (LGN) and from there continue to the primary visual cortex (V1, or striate cortex) first, and to further cortical areas later. The optic chiasm is the point for crossover of information of right and left eyes. The LGN, located at the thalamus, appears to be the first location of feed-forward input from higher levels in the brain to the visual input from the eye before most of the visual input travels to the visual cortex. Note that there is a lateral pathway, that of the superior colliculi, important for eye movement control.

At the visual cortex the signals are processed in V1 and communicated via multiple pathways to numerous visually responsive cortical areas. The visual system comprises a complex network where a cascade of action potentials stream from neuron to neuron forwards, laterally and backwards again. These signals are responsible for our visual perception of the external world, but we are far from understanding how perception of the real world's complex patterns occurs. Visual scientists typically consider that an image can be broken into its components, such as edges, textures, colors, shares, motion, etc. and specialized neurons detect a subset of these components. For a review on receptive field properties of these neurons, retinotopic maps in LGN and V1, orientation and direction selectivity, binocularity and binocular disparity, response timing and other properties of the visual system see online text books (Neuroscience Online, 1997; Webvision, 2011).

## 1.2 Optical aberrations of the eye

In addition to being the main refractive components, the cornea and the crystalline lens are the main sources of aberrations in the human eye. The relative contribution of each of these components can be deduced from total ocular and corneal aberrometry data. The magnitude of the aberration is strongly dependent on individual factors such as age, the state of accommodation or the particular direction through the ocular media. The human eye has monochromatic, longitudinal (up to 2 diopters across the visible spectrum) and transverse chromatic aberrations, the former being significant when using wide bandwidth imaging light sources.

### 1.2.1 Describing human ocular aberrations

The standard representation of ocular aberrations is in terms of Zernike polynomials (American National Standards Institute (ANSI) – 2010). Zernike polynomials are a mathematical series expansion that are orthogonal over a unit circle. Any wavefront profile can be decomposed into a weighted sum of these polynomials. The low order terms can be translated into the common sphere and cylinder notations used in optometric fields (Porter et al, 2006) and are easily corrected using, for example, spectacles or contact lenses. The higher order Zernike polynomials are traditionally not correctable by such methods, although

recently attempts are being made, and require advanced technologies such as AO. Figure 3 shows the first 15 Zernike terms and their corresponding far field point spread functions (PSF).

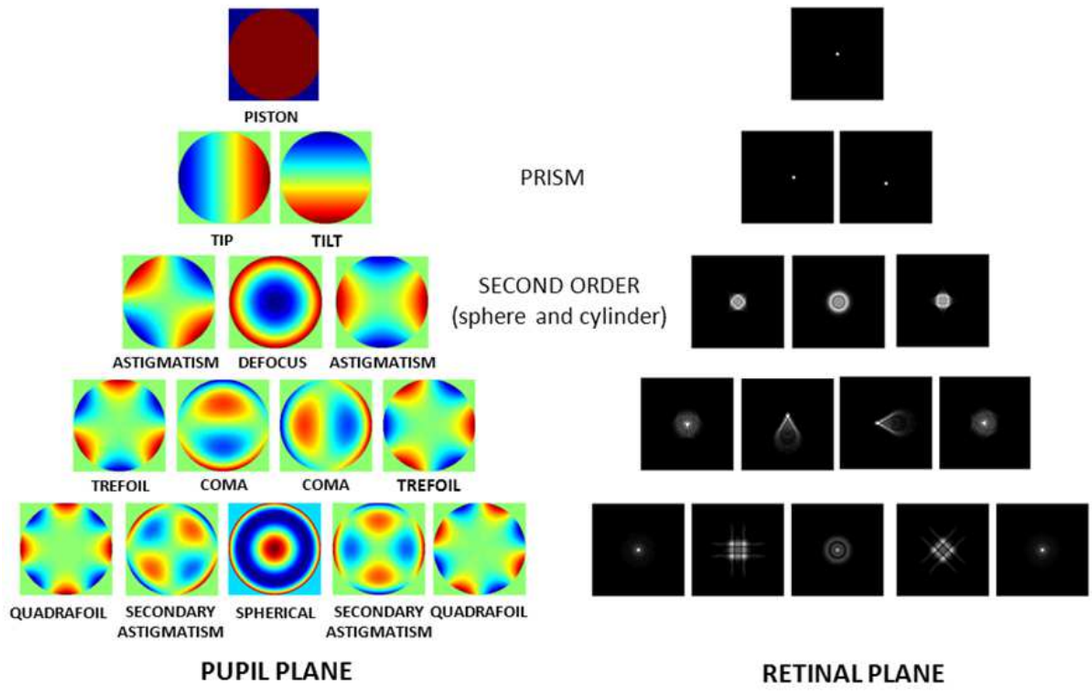


Fig. 3.
(A) The ocular aberrations can be represented as a weighted sum of Zernike polynomials, each representing a specific aberration.
(B) By Fourier transforming and multiplying by the complex conjugate the PSF for each mode can be calculated. Defocus and astigmatism are termed low order modes and are corrected by conventional refractive methods. The higher order modes generally have lower amplitudes but require more elaborate correction technologies.

Porter et al (2001) and Thibos et al (2002) independently measured the wavefront aberration in large human population samples using Shack Hartmann aberrometry. Figure 4 shows measured aberrations coefficients from Porter et al (2001); they measured 109 individuals through a 5.7 mm pupil. The majority of the power lies within the low order modes, i.e. defocus ($Z_2^0$) and astigmatism ($Z_2^{-2}$) and ($Z_2^2$) , with these modes accounting for over 92 % of the total wavefront aberration variance. Note that for this particular study the average defocus coefficient was higher than the general population as they were subjects recruited from a clinic at Bausch & Lomb who were mostly myopic. That said, for high resolution imaging applications where even larger pupil sizes are used, any residual power in the higher order modes can become particularly detrimental.

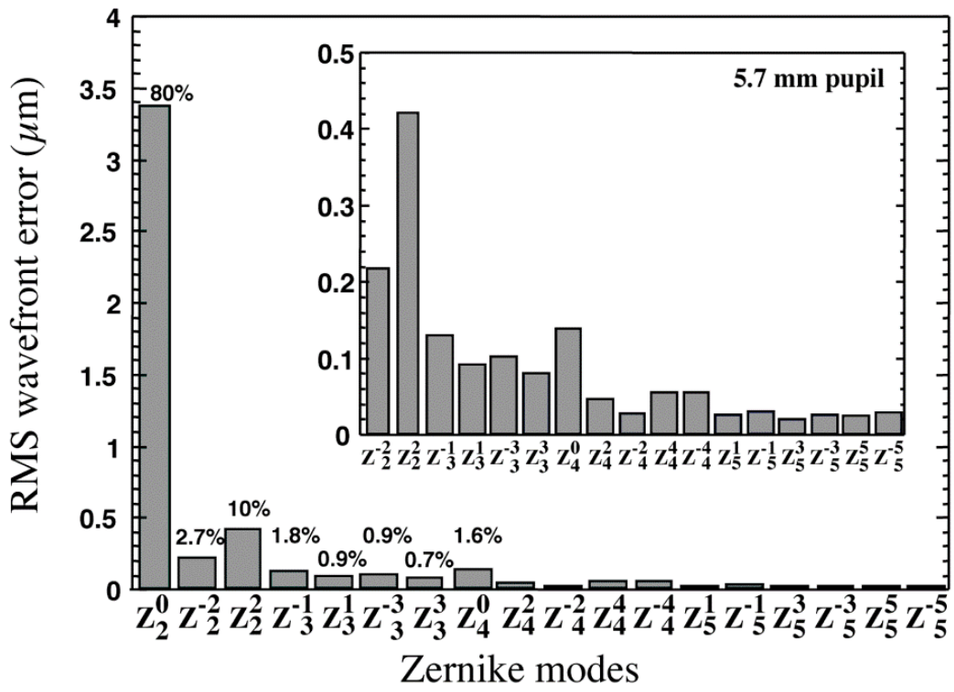


Fig. 4. The wavefront aberration decomposed into Zernike polynomials for a large human population (Porter et al, 2001) over a 5.7 mm pupil. The majority of the aberration power is found in the low order modes, i.e. defocus ($Z_2^0$) and astigmatism ($Z_2^{-2}$ and $Z_2^2$).
The percentages above the first eight modes indicate the percentage of the total wavefront variance. Note: the Zernike order follows that of Noll (1976). Reproduced with permission from the Optical Society of America (OSA).

Doble et al (2007) showed the peak to valley (P-V) wavefront error dependence on pupil size (Fig 5) using aberration data from two human population studies; one comprising of 70 healthy eyes based at the University of Rochester/Bausch & Lomb, and the other consisting of 100 healthy eyes measured at the University of Indiana. Figure 5 shows the wavefront values for each of these populations using different corrective states. Data show that to correct 95 % of the normal human population over a 7.5 mm pupil upwards of 20 μm wavefront correction is required even with the benefit of a second order correction (Fig 5B).

Ocular aberrations also vary with time, mostly due to changes in accommodation (He et al, 2000), although there are other significant contributors such as eye movements. Even when paralyzing accommodation with anticholonergic drugs, the microfluctuations of accommodation can cause significant refractive power changes, up to 0.25 diopters. Hofer et al (2001a; 2001b) and Diaz-Santana et al (2003) have performed detailed measurements on wavefront dynamics and their effect on AO system performance. With a static correction of the higher order aberrations, these dynamic changes can reduce the retinal image contrast by 33 % and the Strehl ratio (SR) by a factor of 3 highlighting the need for real time aberration correction (Hofer et al, 2001b). The SR is defined as the ratio of the peak intensity in the aberrated PSF to that of the unaberrated case; an SR greater than 0.8 is considered to be diffraction limited.

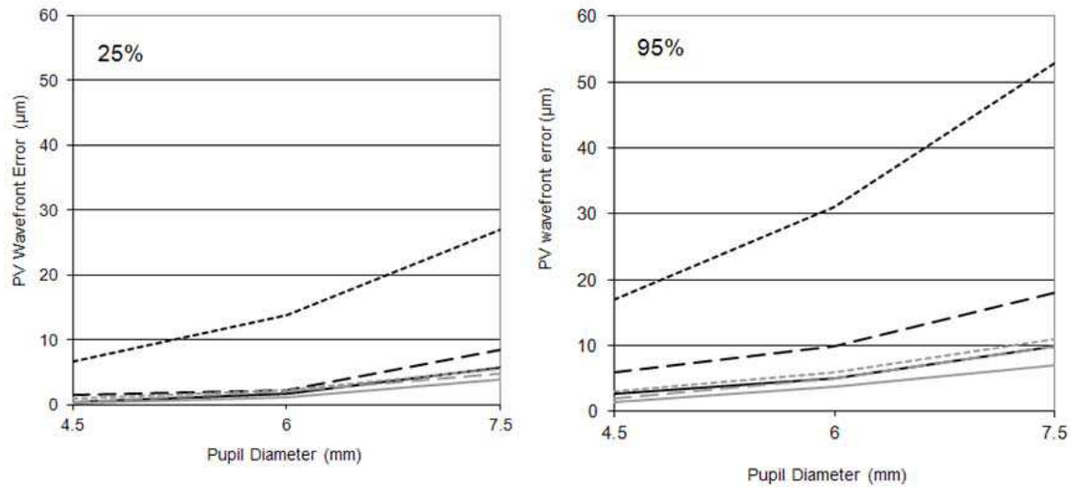


Fig. 5. Peak to valley wavefront error that encompasses 25 (left) and 95 % (right) of the population in the Rochester (black lines) and Indiana (gray lines) populations. For the Rochester data, three correction states are given: (i) all aberrations present (short dashed lines), (ii) all aberrations present with zeroed Zernike defocus (long dashed lines) and (iii) all aberrations present with zeroed defocus and astigmatism (solid lines). For the Indiana data, the three cases are: (i) residual aberrations after a conventional refraction using trial lenses (short dashed lines), (ii) all aberrations present with zeroed Zernike defocus (long dashed lines) and (iii) all aberrations present with zeroed defocus and astigmatism (solid lines) (Doble et al, 2007). Reproduced with permission from the Optical Society of America (OSA).

### 1.2.2 The resolution of the human eye

The lateral (transverse) resolution of the eye is given by Eq. 1:

$$r = 1.22\, f\, \lambda \,/\, n\, D \tag{1}$$

where $r$ is the distance from the center of the Airy disk to the first minima, $f$ is the focal length (of the reduced eye), $\lambda$ is the wavelength, $n$ is the refractive index and $D$ is the pupil diameter. The maximum resolution would be achieved using the shortest wavelength, $\lambda$ and the largest possible aperture, $D$ ($f$ being fixed). As an example, for a human eye, with $D$ = 8 mm, $f$ = 22.2 mm, $n$ ~1.33 and imaging at $\lambda$ = 550 nm, the lateral resolution $r$ is 1.4 µm. In practice, however, ocular aberrations limit this resolution to about 10 µm.

In theory, a lateral resolution of 1.4 µm is sufficient to see the smallest retinal cells. For example, foveal cones have a center to center spacing of 1.9-3.4 µm, and for the rods, the range is 2.2-3.0 µm (Curcio et al, 1990; Jonas et al, 1992). To obtain retinal images with the highest resolution and contrast it is therefore necessary to correct both the low and high order aberrations over a large pupil and moreover track and correct for any associated temporal changes, i.e. we need to employ AO. The ability of AO to dynamically correct (or even induce) higher order spatial modes is becoming increasingly important in the study of the human visual system. The next sections describe how AO is applied to various retinal imaging modalities.

## 2. The application of adaptive optics to the human eye

The concept of AO was first proposed by the astronomer Horace Babcock in 1953 (Babcock, 1953). However, it was not until the late 1960s/early 70s that the first system was implemented, first by the military followed subsequently by the astronomy community. The first step towards the application of AO to the human eye was the work of Dreher et al (1989) who employed a deformable mirror (DM) to give a static correction of astigmatism in a scanning laser ophthalmoscope (SLO). Later work by Liang et al (1994) saw the first use of a Hartmann-Shack wavefront sensor (HS-WFS) for measurement of the human wavefront aberration who then used a HS-WFS in conjunction with a DM (Liang et al, 1997) to produce some of the first *in vivo* images of the cone photoreceptors. Today, AO has been successfully applied to several retinal imaging modalities employing a variety of DM and WFS technologies.

A detailed discussion of AO is beyond the scope of this chapter and the interested reader is referred to the available reference texts (Hardy, 1998; Porter, 2006; Tyson, 2010).

### 2.1 Key AO components

Similar to the AO systems used for other applications such as astronomy and communications, a vision science AO system comprises three main parts:

i. The Wavefront Sensor (WFS): Most vision science AO systems employ a Hartmann-Shack WFS (Shack & Platt, 1971), although curvature (Roddier, 1988) and pyramid sensing (Ragazzoni, 1996) have also been employed successfully to the eye (pyramid sensing: Iglesias et al, 2002; curvature sensing: Gruppett et al, 2005). Typically, the ocular wavefront is sampled at 10-20 Hz with closed loop bandwidths of 1-3 Hz which is sufficient to correct most of the ocular dynamics (Hofer et al, 2001a). The basic operating principle and design considerations of a WFS are the focus of other chapters in this book and will not be discussed here.
ii. The Wavefront Corrector: These are typically DMs although liquid crystal spatial light modulators (LC-SLMs) have been used in several systems (Thibos & Bradley, 1997; Vargas-Martin et al, 1998; Prieto et al, 2004). Early vision AO systems used large, expensive DMs that were originally designed for military, astronomy or laser applications. These DMs had apertures that were several centimeters in diameter requiring long optical paths to magnify the 6-7 mm pupil diameter of the human eye. Today, many systems employ microelectromechanical systems (MEMS) (Fernandez et al, 2001; Bartsch et al, 2002; Doble et al, 2002), electromagnetic (Fernandez et al, 2006) or bimorph type mirrors (Glanc et al, 2004), all of which have much smaller active apertures and a lower cost.
iii. The Control Computer: These take the output of the WFS and converts it to voltage commands that are sent to the wavefront corrector.

There are three main ophthalmic imaging modalities that have successfully employed AO (i) flood illuminated fundus cameras that take a short exposure image of the retina, (ii) confocal laser scanning ophthalmoscopes (cSLOs) that acquire the image by rapidly scanning a point source across the retinal surface and (iii) optical coherence tomography (OCT) which again scans a point source but uses low coherence interferometry to form the image. Each of these modalities are discussed in subsequent sections; however, as the flood illuminated technique is conceptually the simplest it is used here to introduce the application of AO to the human eye.

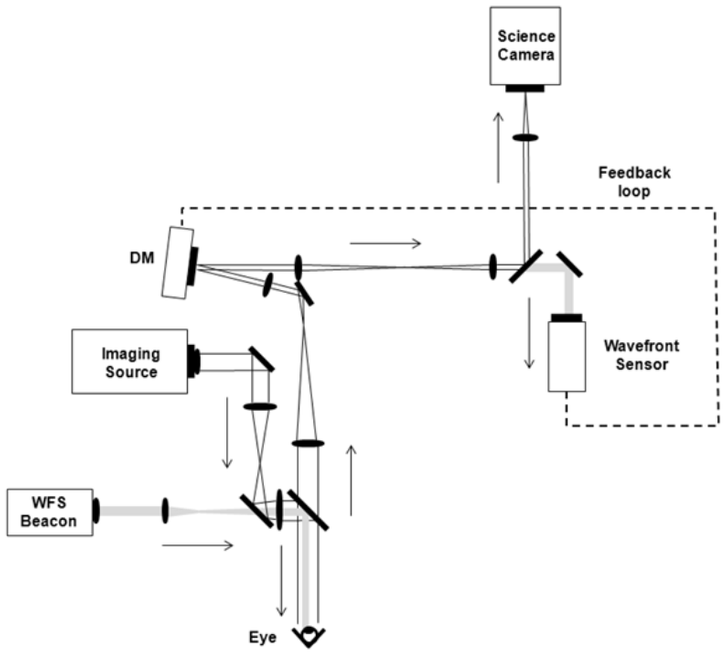


Fig. 6. Schematic of the flood illuminated (flash) AO fundus camera (Headington et al, 2011) in use at the New England College of Optometry.

Figure 6 shows the optical layout of the New England College of Optometry (NECO) AO flood illuminated (flash) fundus camera (Headington et al, 2011). The WFS beacon is used to measure the ocular aberration, a small incident beam (1mm diameter at the cornea) from a superluminescent diode (SLD) at 820 nm is focused to a ~10 μm diameter spot on the retina. The scattered light exits through the dilated pupil (6mm in diameter) and is redirected by the DM, through the dichroic beamsplitter into the WFS. The aberrations are sampled at 20 Hz and the required correction profile is sent to the DM. The system is fast enough to track and correct dynamic ocular aberration changes at a frequency of ~1 Hz. As with all AO systems used in vision, the DM and the WFS are placed in optical planes approximately conjugate to the pupil of the eye. Once the aberrations have been corrected, typically below 0.1 μm rms over the 6mm diameter pupil, the retinal image is acquired. The imaging source is usually an arclamp and delivers a 4-6 msec retinal exposure. The particular imaging wavelength (between 500-800 nm) is chosen to highlight a particular retinal feature. The imaging light follows the corrected path through the AO system and is redirected to the science camera via a dichroic beamsplitter. Typical retinal image sizes are 1-3$^{o}$ (0.3-0.9 mm diameter).

The system described in Figure 6 can be easily modified for functional vision testing. The science camera can be replaced by a visual test pattern, such as a visual acuity or a contrast sensitivity chart. The projected test image is then pre-distorted by the conjugate ocular aberration before being incident on the retina – see later section titled AO for Vision Testing.

### 2.2 Light level considerations

It is essential in the operation of any ophthalmic device that the light levels used are safe. The wide range of imaging modalities, frame rates, wavelengths, field sizes and exposure

durations mean that the maximum permissible exposures (MPE) must be calculated on a case by case basis. Several reference standards are used in such calculations (ANSI, 2007; Delori et al, 2007).

### 2.3 Wavefront corrector requirements

Independent of the particular imaging modality, the benefit of AO in ophthalmic systems fundamentally relies on its ability to measure, track and correct the ocular aberrations. It is therefore imperative that the WFS, and in particular the wavefront corrector, have optimal operating characteristics. As DMs are the most commonly used form of wavefront corrector their performance is described in detail here. LC-SLMs (Li et al, 1998) can be modeled as piston-only DMs.

DMs can be divided into two broad categories, continuous surface and segmented (Fig 7). In both cases, there is a set of actuators that physically deform the mirrored surface. Examples of actuation mechanisms can be electrostatic, piezoelectric, magnetic, thermal or voicecoil. Refer to Tyson (2010) for more details on the various types of DMs and their actuation mechanisms. Figure 7A shows a cross section through a continuous surface DM. A two dimensional array of actuators deforms the surface. The greater the number of actuators the higher the spatial frequency correction capability. Light would be incident from the top of the figure. Figure 7B shows a segmented piston/tip/tilt (PTT) DM. In this case, each segment has three degrees of freedom. A common variant is a piston only DM in which an individual segment can only move in the vertical direction. For a continuous surface DM adjusting one actuator causes a deformation of the top mirrored surface and the degree of localization is termed the influence function. Certain DM types, such as membrane and bimorph, have very broad influence functions meaning that activation of one actuator causes a deformation over a large area of the DM. Segmented DMs however have much narrower influence functions; moving a piston only segment only changes that segment's mirror position and not that of its neighbours. The shape of this influence function, along with the number of actuators and the dynamic range, define the corrective ability of a DM.

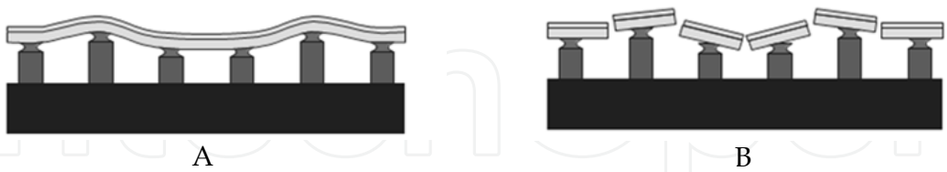


Fig. 7. Deformable mirror (DM) types. (A) Continuous surface mirror, deformed by an underlying array of actuators. (B) Segmented surface - the mirror is composed of a discrete array of segments each of which has three degrees of freedom: piston, tip and tilt (PTT). Piston only segmented DMs are also possible.

Figure 8 shows the DM correction performance as a function of the number of actuators or segments across a 7.5 mm pupil for a 0.6 μm wavelength. The Rochester population dataset described earlier (Fig 5), was analyzed after zeroing the defocus coefficient. For continuous surface DMs approximately 15 actuators are required to give diffraction limited performance (SR > 0.8), with 12 segments giving the same performance for PTT devices

(with the caveat that three times as many control voltages are required to move one segment as compared to a single actuator). Piston only DMs require many more segments to achieve good correction with over 100 being necessary; however, these numbers are easily achievable with newer LC-SLMs.

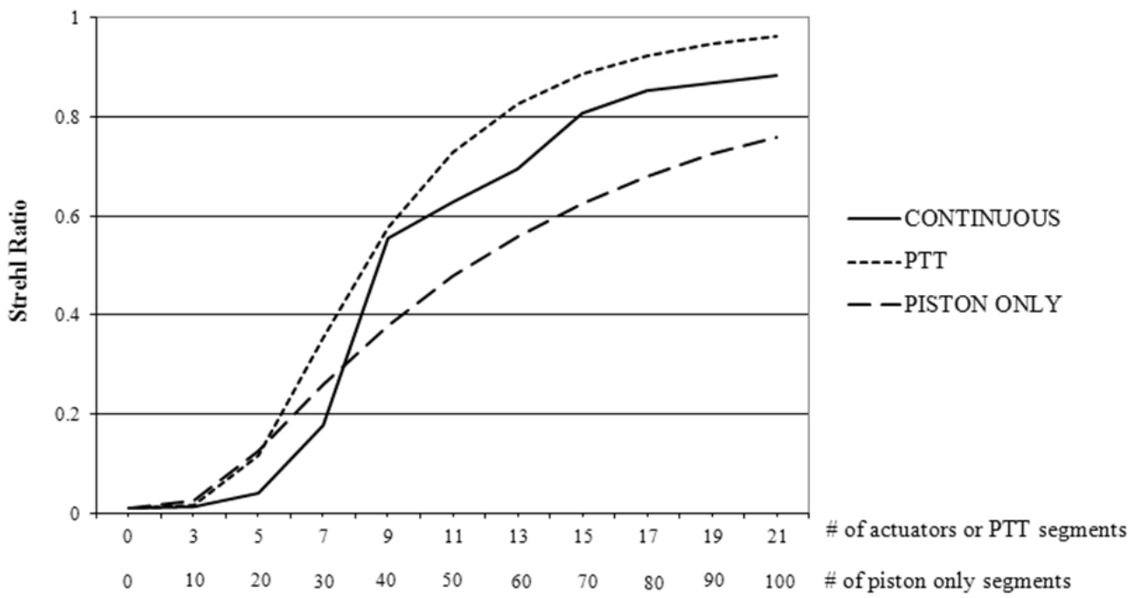


Fig. 8. DM correction performance as a function of the number of actuators or segments after zeroing the defocus coefficient. Continuous (solid line) or PTT segmented (short dashed) DMs have comparable performance with 12-15 actuators or segments being required to achieve a SR of 0.8.

## 3. AO modalities and applications in ophthalmic imaging

AO improves the capabilities of any ophthalmic instrument where the optics of the eye are involved, from fundus cameras to phoropters. With the high lateral resolution achievable through the use of AO, as described above, it is now possible to detect the earliest changes caused by retinal pathologies. Small structures, such as the smallest microaneurism (early signs of diabetic retinopathy), blood cells, photoreceptor cells, ganglion cells, RPE cells, the smallest capillaries and cells' organelles can now be observed with the high resolution achievable by AO imaging (e.g. Roorda & Williams, 1999; Roorda et al, 2007; Chen et al, 2011; Wang et al, 2011; Zhong et al, 2011). A number of laboratories and clinical centers have begun to evaluate eye diseases using AO imaging. Choi et al (2006) and Wolfing et al (2006) first reported *in vivo* images of photoreceptors in a patient with rod-cone dystrophy, which revealed a reduction in cone density. It has also been shown that retinitis pigmentosa and rod-cone dystrophy show a different pattern of cone degeneration (Duncan et al, 2007). Congenital color deficiencies have been studied using AO imaging (e.g. Carroll et al, 2004; Rha et al, 2010)). Choi and colleagues found that AO imaging is a reliable technique for assessing and quantifying the changes in photoreceptors in a number of optic neuropathies (Choi et al, 2008) and glaucoma (Choi et al, 2011). AO imaging has also proven to be useful

in patients with inherited Stargardt's disease (Chen et al, 2011). Marmor et al (2008) used AO as well as conventional OCT to evaluate the visual significance of the foveal pit and found that it is not required for the specialization of foveal cones. More recently, McAllister et al (2010) have found variation in the degree of foveal hypoplasia and the corresponding variation in foveal cone photoreceptor specialization.

### 3.1 Flood illuminated (Flash) AO fundus cameras

The first AO retinal imaging systems were flood illuminated designs as depicted in Figure 6. They are extremely versatile and may be configured for a variety of imaging and vision testing experiments. Their disadvantage for imaging is that they are susceptible to ocular scatter as all of the reflected light is imaged onto the science camera, thus reducing imaging contrast, and they have essentially zero axial resolution. In addition, they tend to be slow with sub-Hertz image acquisition rates, although video rate systems have also been built (Rha et al, 2006).

In 1996, Miller et al (1996) obtained the first *in vivo* images of the cone receptors using a high resolution flood illuminated fundus camera (coupled with a precise second-order refraction). The introduction of a full AO system by Liang and Williams (1997) further enhanced the contrast and quality of the cone images. Since then many other flood AO systems have been built (e.g. Hofer, 2001b; Larichev et al, 2002; Glanc et al, 2004; Choi et al, 2006; Rha et al, 2006; Headington et al, 2011). They have utilized improved AO components and imaged a variety of retinal structure and function in both normal (e.g. Roorda & Williams, 1999, 2002; Pallikaris et al, 2003; Putnam et al, 2005; Jonnal et al, 2007; Doble et al, 2011) and diseased eyes (e.g. Carroll et al, 2004; Choi et al, 2006, 2008, 2011; Wolfing et al, 2006; Carroll, 2008).

### 3.2 Adaptive Optics Confocal Scanning Laser Ophthalmoscopes (AO-cSLO)

In a cSLO, a point of light is scanned rapidly across the retina in a two-dimensional transverse pattern. The reflected light passes through a pinhole that is confocal to a particular retinal layer. This light is then incident on a point detector such as a photomultiplier tube (PMT) or avalanche photodiode (APD). The two dimensional image can then be reconstructed from the detector output. This approach has two major advantages: (i) reduced scattering as only light from a particular point and retinal layer passes through the confocal pinhole (all other light is blocked) and all other light is blocked, and (ii) it allows for video rate imaging of retinal structure and processes.

The two dimensional scan is achieved in modern systems through the use of a fast-mirrored resonant scanner and a slower galvanometric frame scanner; typical frame rates are 20-30 Hz. The field of view is similar to flood-based AO systems (1-3$^{o}$). Standard cSLOs have transverse and axial resolutions of approximately 5 µm and 200 µm respectively, but through the use of AO the resolution is improved to 2.5 µm transversely and <80 µm axially; with these numbers being dependent on the pupil size and imaging wavelength used.

In 1980, Webb and his colleagues (1980) demonstrated the first SLO, which was followed by the work of Dreher et al (1989) who used a DM in conjunction with an SLO. Wade and Fitzke (1998) used an SLO and post-processing to visualize the cone photoreceptors. The

first closed-loop AO-cSLO was developed by Roorda et al (2002). Newer systems have pushed the performance even further allowing for the use of dual DMs (Chen et al, 2007a), increased fields of view (Ferguson et al, 2010) and the ability to visualize the rod photoreceptors (Dubra et al, 2011; Merino et al, 2011). For further details the reader is directed to the chapter on AO-cSLOs.

### 3.3 Adaptive Optics Optical Coherence Tomography (AO-OCT)

Optical coherence tomography (OCT) (Huang et al, 1991; Fercher et al, 1993; Swanson et al, 1993) is a non-invasive imaging modality that exploits the coherence properties of light to form an image. A light source is split into a reference channel and a sample channel via a modified Michelson interferometer. The retinal surface located in the sample channel is rapidly scanned and the reflected light interferes with that of the reference arm. Axial or 'A-scans' are generally acquired first allowing for the subsequent construction of the commonly displayed 'B-scans'. Three-dimensional volume scans can then be created. A major advantage of OCT is the axial and lateral resolutions are decoupled. The axial resolution depends on the bandwidth of the light source, the broader the bandwidth the higher the resolution, although compensation of the chromatic aberration of the eye is then required (Fernandez et al, 2005; Zawadzki et al, 2008). Axial resolutions of a few micrometers are possible. The lateral resolution is a function of the pupil size which in turn influences the level of aberration, hence the need for AO.

The first systems combined AO with OCT (Miller et al, 2003; Hermann et al, 2004; Zhang et al, 2005), more recently we are seeing the emergence of systems with multimodal imaging capabilities, AO-OCT-SLO systems (Iftimia et al, 2006; Merino et al, 2006; Miller et al, 2011; Zawadzki et al, 2011).

## 4. AO for vision testing

Human visual performance is limited by neural (retinal or at higher visual level) and optical factors. The evaluation of the contribution of each of these factors has proven difficult in the past, since the study of one was confounded by the other and vice versa. Prior attempts to separate the effect of these limiting factors included interferometry and the detection of contrast in images embedded in noise, however both methods have significant procedural limitations.

The use of AO for correcting aberrations in the human eye opened the possibility of evaluating the effect of neural factors since the optical effects are compensated for. Soon after the first applications of AO to obtain high-resolution images of the retina (Liang et al, 1997), a number of laboratories began exploring the use of AO to produce aberration-free retinal images to improve vision and evaluate visual function. It was shown that the correction of aberrations improved the contrast sensitivity function (CSF), showing sensitivity at frequencies up to 55 cycles per degree, not possible without AO correction (Liang et al, 1997), and improved the visual system's resolution or VA (Yoon & Williams, 2002). AO has also been used to modify the aberrations of the eye to study visual performance (Artal et al, 2004; Chen et al, 2007b). The limiting factor once aberrations are corrected with AO is the sampling of the photoreceptors. Positive effects of the correction of aberrations have been shown in other functions such as face recognition (Sawides et al, 2010) and even some improvement in the periphery of the visual field, where optics do not

play such an important role (Roorda, 2011). These results seemed to imply that correcting aberrations, e.g. with refractive surgery, would significantly improve visual performance. However, since the eye is a living organ and the visual system ever changing, there are potentially significant limitations to the benefit of high order aberration correction to visual function as we describe below.

i. Accommodation

Accommodation is the process of changing the power of the eye by modifying the shape and position of the crystalline lens. The amount of accommodation required to form a clear retinal image is controlled by a number of cues, most of which are related to the retinal stimulus quality, such as blur and chromatic aberration, although some, e.g. retinal disparity and proximity, are not.

AO has allowed further evaluation of the stimuli that drive accommodation and disaccommodation, which seem to be non-parallel processes. Among the possible cues that may indicate the sign of defocus to drive accommodation are higher order monochromatic and chromatic aberrations. A number of authors have studied accommodation and disaccommodation with the manipulation of high order aberrations (Hampson et al, 2006; Chin et al, 2009a; Hampson et al, 2010) and suggested that aberrations play a role in the accommodation control of dynamic (stepwise and sinusoidal) stimuli. However, there is controversy as to the role of aberrations in accommodation since other authors have found improvement rather than a reduction of accommodation when correcting aberrations (Gambra et al, 2009). Further work is needed to determine the role of higher order aberrations in accommodation. Aberrations may play a role in the time response of accommodation rather than its accuracy (Fernandez & Artal, 2005).

Presbyopia, the decreased ability of the eye to accommodate as it ages, may also benefit from AO aberration correction (see section below on the correction of refractive error using AO).

ii. Refraction and Refractive Technologies Using Wavefront Sensing and AO Correction

Autorefractors are computer-controlled instruments that provide objective measurement of the eye's refractive error by measuring the vergence of the light reflected from the retina. They are often used by eye care professionals as a starting point for a subjective refraction. The use of clinically available aberrometers (e.g. Ophthonix Z-View aberrometer; Huvitz HRK-7000AW autorefractor/aberrometer) that measure higher order as well as lower order aberrations instead of the traditional autorefractor are becoming more popular as they have shown greater accuracy (Cooper et al, 2011). A spectacle correction based solely on the measures obtained from these instruments is not appropriate in most patients as they tend to overcorrect astigmatism – and some myopia - and give high errors when determining the axis for low astigmatic magnitudes. A phoropter is an instrument that contains lenses typically used by eye care professionals for subjective refraction of the eye typically used during an eye examination, i.e. correction of the lower aberrations – defocus and astigmatism. Phoropters incorporating AO would correct for higher order aberrations in addition to defocus and astigmatism using the wavefront pattern obtained with the aberrometer as a base and a subjective refraction as an endpoint.

AO vision simulators may also be useful tools to help finding the best refractive prescription for patients. Rocha et al (2010) used a crx1 AO Visual Simulator (Imagine Eyes SA) to correct

and modify the wavefront aberrations in keratoconic eyes and symptomatic postoperative refractive surgery (LASIK) eyes. The AO visual simulator correction improved visual acuity by an average of two lines compared to their best spherocylinder correction. The AO technology may be of clinical benefit when counseling patients with highly aberrated eyes regarding their maximum subjective potential for vision correction.

Lower order aberrations, i.e. defocus and astigmatism, have been measured for hundreds of years and are typically corrected with spectacles, contact lenses, intraocular lenses or refractive surgery. The emerging AO technologies and the improvement in visual performance found with the correction of higher order aberrations has brought excitement to the field of refractive error correction. During the last decade there has been considerable debate concerning the visual impact of correcting the higher order aberrations of the eye.

First attempts to correct higher order aberrations used spectacle lenses and contact lenses. Both of these designs do not benefit significantly from correction of high order aberrations as aberrations are not constant but change with off-axis viewing, movement of the device, pupil size changes and accommodation, among other factors (Lopez-Gil et al, 2007). The use of scleral contact lenses helps with the stability problem of conventional contact lenses. A practical use of these lenses (Sabesan et al, 2007; Katsoulos et al, 2009; Sabesan & Yoon, 2010) for correction of the particularly elevated aberrations found in keratoconus seems plausible. Most of the difficulties found with spectacle lenses and contact lenses may be compensated if other methods of aberration correction, such as refractive surgery or intraocular lenses, are used.

AO has been applied in multifocal intraocular lenses for the correction of presbyopia as it extends the depth of focus by varying the amount of spherical aberration for axial (small pupil) rays for near vision and peripheral rays (larger pupils) for distance. Spherical aberration can be significantly reduced with aspheric intraocular lenses; however, there is a limited reduction in the total high order aberrations, even in perfectly positioned custom aspheric intraocular lenses, which may be influencing the unclear results in the studies assessing the potential benefits on visual performance of these lenses (Einighammer et al, 2009). AO has also been used to show that accommodative intraocular lenses for the correction of presbyopia actually work via pseudoaccommodative rather than accommodative mechanisms (Klaproth et al, 2011).

Refractive surgery has traditionally corrected lower order aberrations. Conventional refractive surgery may disrupt the compensation mechanism of corneal and internal ocular aberrations, creating a larger total amount of high order aberrations (Benito et al, 2009). With the advances in wavefront sensing technology, customized refractive surgery is common nowadays. Compared with conventional treatments, wavefront-guided ablations can achieve a reduction in preexisting higher-order aberrations and less induction of new higher-order aberrations, resulting in improved outcomes for contrast sensitivity and visual symptoms under mesopic and scotopic conditions (Kim & Chuck, 2008). However, concerns regarding the clinical applicability of customized wavefront correction have emerged, and the possibility of achieving supernormal vision in all patients has been challenged (e.g. Yeh & Azar, 2004).

The results of the reviewed studies suggest that many, but not all, observers with normal vision would perceive improvements in their spatial vision with customized (AO) vision

correction, at least over a range of viewing distances, particularly when their pupils are larger than 3 mm. Keratoconic patients and patients suffering from high spherical aberration, e.g. as a result of conventional refractive surgery, would particularly benefit (Rocha et al, 2010). A recently developed technique combining customized (topography-guided) refractive surgery with riboflavin/UVA cross-linking seems a promising development for the treatment of progressive keratoconus (Krueger & Kanellopoulos, 2010).

iii. Using an AO-cSLO as a High-Frequency Eye Tracker

While the first attempts were made to correct the distortions found in the SLO frames due to eye movements, it was realized that these data are a record of the movements that had occurred during acquisitions. Therefore, the eyes can be tracked with an accuracy and frequency that would not be achieved with the best eye trackers available (Roorda, 2011).

iv. Simultaneous Stimuli Presentation and Image Delivery

With a cSLO the stimulus can be directly encoded in the rastered image, giving a real-time exact position of the stimulus in relation to the surrounding cones. Furthermore, with the incorporation of AO, the stimuli may be delivered to precise regions of the retina, to the level of individual photoreceptors (Sincich et al, 2009). Using a different channel for imaging and stimulus delivery, an infrared light may be used to image the retina while a visible light is used to present the stimuli and be used to record processes occurring at the retinal level as explained in the visual function section below. This technology can also be applied to fluorescence imaging to allow evaluation of sensitivity of non-absorbing structures such as axonal and dendritic structures of primate ganglion cells *in vivo* (Gray et al, 2008). The axial and lateral resolution achieved with AO was high enough to visualize individual dendrites and axons and was able to distinguish between ganglion cell types and function.

Still images and animations can also be delivered into a specific locus at the retina. Surprisingly, moving and stationary targets seem to generate different fixation loci and neither is correlated with the point of maximum cone density (Putnam et al, 2005; Stevenson et al, 2007).

AO-cSLO technology has also the potential for presenting stimuli at the level of a single photoreceptor and performing microperimetry – i.e. measure sensitivity - at an unprecedented degree of retinotopic precision (Makous et al, 2006; Tuten et al, 2011). Such technology would be very useful in studies determining the preferred locus of fixation (Putnam et al, 2005; 2011) and its relation with photoreceptor density. The preferred locus of fixation is an important parameter to obtain in patients with eccentric fixation and in patients with low vision who have central vision loss, e.g. caused by macular degeneration.

v. Visual Acuity and Contrast Sensitivity

By modifying an existing AO imaging device (fundus camera, SLO), stimuli may be imaged onto the retina without aberrations or with a controlled amount/type of

aberrations. In addition to work by Liang et al (1997), Yoon and Williams (2002) also used AO to measure VA and contrast sensitivity (CS) through an aberration-corrected eye, with the limiting factor being the sampling of the photoreceptors, and found improved VA and CS at spatial frequencies of 16 and 24 cycles/deg. Most but not all observers showed improvement in VA and CS (e.g. Elliott & Chapman, 2009). Rossi et al (2007) found that myopes do not perform as well after AO correction as emmetropes; it was suggested that this difference is not due to larger cone spacing, as axial myopes (longer eyes) do not show smaller sampling than emmetropes (Li et al, 2010).

vi. AO Imaging Correlations with Visual Function

A number of reports have shown correlation between AO retinal imaging and visual function tests. Choi et al (2006) first reported that disruption of the cone photoreceptors mosaic in patients with various forms of retinal dystrophies is correlated to functional vision losses (visual fields, contrast sensitivity and and multifocal electroretinography – mfERG) (Fig 9). In toxic maculopathy caused by hydroxychloroquine (antimalarial drug used extensively in the treatment of autoimmune diseases), AO ophthalmoscopy also shows disruption of the cone photoreceptor mosaic in areas corresponding to visual field defects, and shows additional areas of irregularities in cone photoreceptor density in areas with otherwise normal visual field findings, suggesting that AO imaging is detecting changes earlier than visual field tests (Stepien et al, 2009). AO-cSLO imaging of the cone mosaic explained visual performance, a unilateral ring-like paracentral distortion that could otherwise not be explained using common clinical imaging instruments (Joeres et al, 2008).

More recently, Talcott et al (2011) has found that the use of AO imaging was more useful than the standard of care tests for evaluation of the effect of treatment in three patients with retinal degeneration. Furthermore, AO-cSLO has been used to evaluate cone spacing in familial mitochondrial DNA mutation. Visual function was affected with various levels of severity depending on the cone spacing pattern; it was improved in patients with a contiguous and regular cone mosaic. Patients expressing high levels of the mitochondrial DNA mutation T8993C showed abnormal cone structure, suggesting normal mitochondrial DNA is necessary for normal waveguiding by cones (Yoon et al, 2009). High resolution AO imaging and AO for visual function evaluation of photoreceptors have also been proven useful techniques in selection of patients for therapeutic trials of congenital achromatopsia and for monitoring the therapeutic response in these trials (Genead et al, 2011). AO fundus imaging has also been used to investigate photoreceptor structural changes in eyes with occult macular dystrophy (Kitaguchi et al, 2011). Furthermore, high resolution imaging with AO-cSLO has contributed significantly to our understanding of Stargardt's disease, a disease that severely affects central vision of young, otherwise healthy, individuals. AO-cSLO imaging showed abnormal cone spacing in regions of abnormal fundus autofluorescence and reduced visual function, although the earliest cone spacing abnormalities were observed in regions of homogeneous autofluorescence and normal visual function (Chen et al, 2011). In addition, visual resolution decreases rapidly outside the foveal center towards the peripheral retina, which seems to be more related to sampling of midget retinal ganglion cells than photoreceptor sampling (Rossi & Roorda, 2010b).

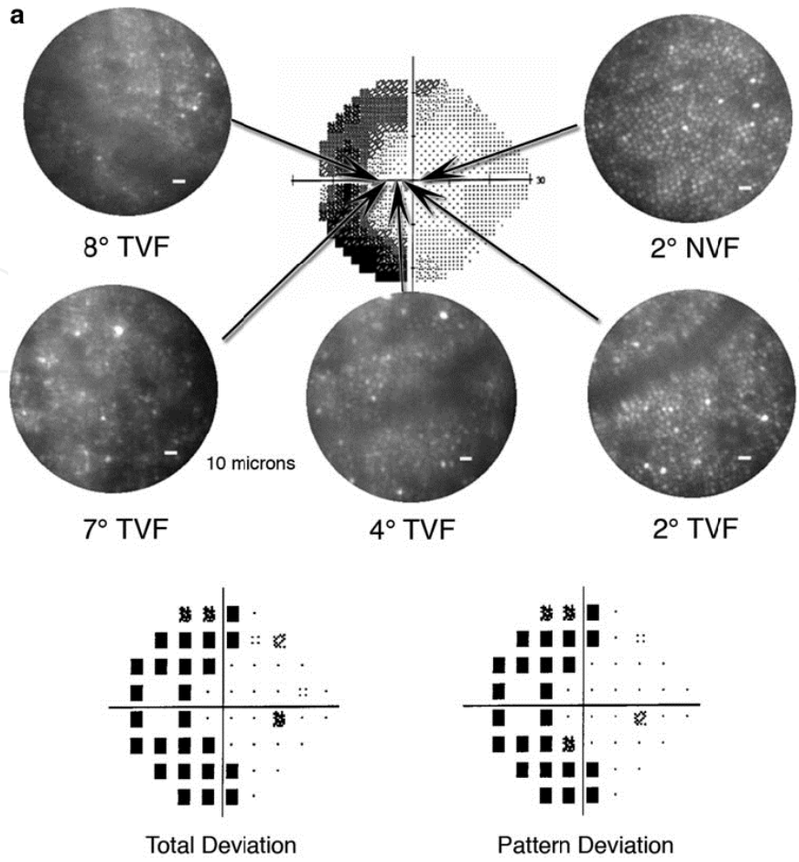


Fig. 9. AO-corrected retinal images for a subject with a retinal dystrophy at different locations of the retina shown with the corresponding visual field maps. Reprinted from Choi et al (2006), with permission from the journal Investigative Ophthalmology and Visual Science.

These studies indicate that AO fundus imaging is a reliable technique for assessing and quantifying the changes in the photoreceptor layer as the disease progresses. Furthermore, AO imaging correlates with visual function tests and may be useful in cases where visual function tests provide borderline or ambiguous results, as it allows visualization of individual photoreceptors. Some caution is warranted as there may be greater higher-order wavefront aberrations in eyes with macular disease than in control eyes without disease (Bessho et al, 2009). It has been suggested that portion of the aberration measurements may result from irregular or multiple reflecting retinal surfaces.

vii. Visual Perception at the Photoreceptor Level

AO systems are unique in that they provide structural and functional information of the visual system and therefore allow a new class of experiments with great scientific potential. For example, testing of image perception at the level of an individual photoreceptor is now possible with the use of AO. Roorda and Williams (1999) were the first to show *in vivo* images of the arrangement of the human trichromatic arrangement. By bleaching the retina with three different wavelengths they were able to classify the individual cones according to their photopigment type. The relative numbers of L and M cones varied significantly among subjects, even though all had the same color perception.

Using AO-cSLO, Sincich et al (2009) were able to deliver micron-scale spots of light to the centers of the receptive fields of neurons in the macaque LGN and resolve the contribution of single cone photoreceptors to the response of central visual neurons. They imaged and directly stimulated individual cones in the macaque in vivo, while neuron receptive fields were recorded in the LGN. It is therefore possible to now study the properties of different photoreceptors and their influence in visual perception.

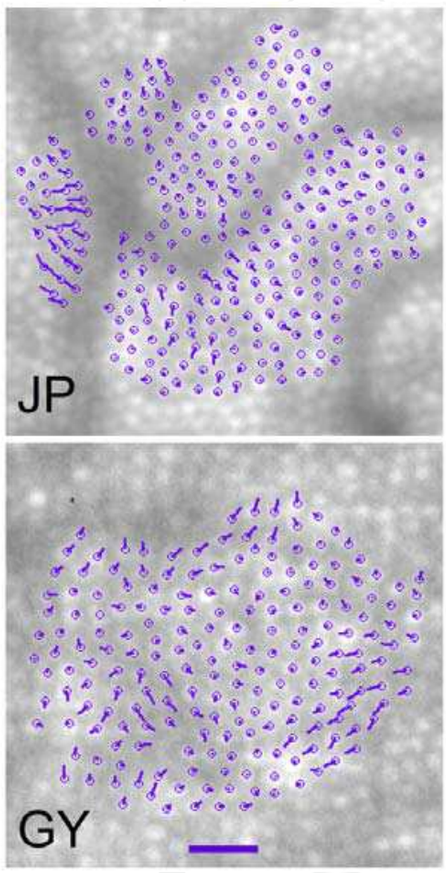


Fig. 10. Cone directionality plots for two subjects, from Roorda and Williams (2002). The circles represent cone locations and the lines the direction and magnitude of the departure of each cone's pointing direction in the pupil plane from the average of the ensemble. Reprinted with permission from the Journal of Vision.

As mentioned in the first section of this chapter, Roorda and Williams (2002) imaged the angular tuning properties (SCE) of individual photoreceptors in living human eyes. They found that the disarray in macular cones is very small, implying that the optical waveguide properties of ensembles of cones are similar to those of the single cones that compose them (Fig 10).

## 5. Ongoing challenges in applying AO for vision

Controlling and correcting aberrations allows the possibility of exploring their effects on human vision and their correction may improve visual performance. However, questions regarding the real benefits of totally eliminating aberrations remain (e.g. Chen et al, 2007b).

The subjective image quality depends on intrinsic optical (e.g. aberrations) and neural factors (Campbell & Green, 1965), as well as the prior experience of the observer. One of the neural limits is adaptation to blur (e.g. Georgeson & Sullivan, 1975; Webster et al, 2002; Vera-Diaz et al, 2010). Adaptation to blur is well known by eye care professionals as their myopic patients often report clearer vision after a period of not wearing their spectacles. Adaptation seems to occur not only for defocus and astigmatism (de Gracia et al, 2011), and other types of induced blur, but the visual system seems to also be adapt to the eye's own high order aberrations profile (Artal et al, 2004; Sawides et al, 2011), somehow removing the effects of blur induced by the optics of the eye. Best subjective image quality is obtained when some amount (~12 %) of high order aberrations are left uncorrected (Chen et al, 2007b). Further, observers seem to prefer a small amount of positive spherical defocus for best visual performance (Werner et al, 2009). Adaptation may have important implications in the correction of aberration with customized refractive surgery or contact lenses, as the benefits of that correction may be overcome with neural adaptation. However, the effect may disappear after adaptation to the new level of aberrations. Rossi and Roorda (2010a) have suggested that adaptation to aberrations does not hinder the correction with AO from giving immediate visual benefit since AO provided a significant improvement in visual resolution, and visual resolution is a low level task that is not expected to improve with training. It is yet to be determined whether the improvement found in static laboratory measures of VA and CS corresponds to an improvement in real life visual tasks. Furthermore, the improvement in these measures seems to be only found with larger pupil sizes (Elliott & Chapman, 2009) which do not occur in natural viewing. It also seems that the presence of aberrations is utilized as a cue by the visual system for accommodation (Kruger et al, 1993; Chen et al, 2006; Chin et al, 2009b) and perhaps for control of other oculomotor functions of the eye. Therefore, correcting these aberrations may negatively interfere with these visual functions.

In addition to neural limitations, the image quality presented to the retina has other optical dependencies besides aberrations; for example, ocular media density and light scatter, as well as diffraction (the eye is a diffraction-limited optical system at small pupil diameters). These are neither measured nor corrected by AO. Visual function, for example VA and CS at mid- and high-spatial frequencies, is compromised with normal aging. Elliott and Chapman (2009) found that increased high order aberrations that occur with aging (due to coma induced by asymmetric corneas, spherical aberration caused by changes in the lens, etc.) cannot completely account for the decline in spatial vision with aging. A larger role of the aforementioned optical factors and, perhaps more importantly, neural factors, exists in changes in spatial vision found with aging. Elliott et al (2007) and Vera-Diaz et al (2010) found no difference in the strength of adaptation to transient changes in image blur for younger and older observers, suggesting that cortical mechanisms of adaptation remain largely intact with age and could provide a mechanism for long-term adaptation to the increasing degree of high order aberrations with age.

Furthermore, ocular aberrations are dynamic, as explained above, and vary with eye movements, accommodation, etc., which bring subsequent limitations to the benefit of aberration correction.

Other potential limitations to the use of AO for vision science and clinical care are that these devices are not yet user-friendly and are cumbersome, although compact devices are being

developed (Mujat et al, 2010). It has also been recently suggested that there are potential differences between AO fundus camera images and AO-cSLO images (Carroll et al, 2010), which requires further investigation. In addition, there are a number of technical limitations of AO systems that require further work. For example, during the time it takes to capture an image with an AO-cSLO device (about 30 msecs), the eye moves significantly and in unpredictable ways causing distortions in each frame. These distortions can be corrected for, but this is a work in progress.

## 6. The future of AO in vision science

In spite of the limitations described in the previous section, ophthalmic systems that employ AO have the potential to play a crucial role in the clinic. Although the use of AO in clinical settings is still to come, primarily because of the cost and the time-consuming nature of the testing and data processing, the recent substantial and rapid advances of these technologies suggest that their commercialization for ophthalmic clinical use is imminent. A number of prototypes are currently being tested. The AO fundus camera developed by Imagine Eyes © (rtx1™ Adaptive Optics Retinal Camera) is currently commercially available, for research use only, not for sale as a diagnostic device, and clinical trials began in France in 2009 and it may be available soon for clinical use. Physical Sciences Inc. has developed AO imaging devices and an AO-cSLO system, again for research only.

Noteworthy applications of AO imaging are the evaluation of the longitudinal progression of a disease and the evaluation of treatment efficacy. Further insight on the progression of retinal diseases is fundamental for understanding the molecular basics of these diseases. Likewise, the evaluation of the disease response to novel treatments with accurate objective methods such as AO imaging is far more informative than current subjective evaluation methods (e.g. VA and CS), and is critical for determining treatment efficacy. Retinal diseases are in general of slow progression, with some taking several years before changes in functional vision may be appreciated; however, disease progression has been shown with AO imaging techniques. With the use of AO it is now possible to image the smallest structures of the eye *in vivo*; not only retinal cells, but organelles and other microscopic structures are being imaged. As a result of the high transverse resolution of OCT and lateral resolution of SLO with AO, these evaluation measures are quickly being adopted as clinical trials' endpoints.

Talcott et al (2011) has recently completed the first longitudinal study of cone photoreceptors during retinal degeneration (in patients with inherited retinal degeneration, such as retinitis pigmentosa and Usher syndrome) and evaluated the response to a treatment with a ciliary neurotrophic factor. Changes in functional tests such as VA, CS and mfERG were monitored over 2 years. AO-cSLO images showed reduced cone loss in patients treated compared to the contralateral sham eyes (Sincich et al, 2009). Longitudinal studies on healthy eyes are necessary to create a database of normative data against which to compare disease data.

AO vision simulators may become useful tools to help choose the best refraction for patients. Clinicians will be able to show their patients what their vision would be like if they undergo a particular method of refractive surgery compared to another or compare between various kinds of intraocular lenses. Patient education could benefit from these simulators, particularly with the increased interest in presbyopic surgery, or the use of multifocal contact lenses, as patients may better understand and experiment with the visual benefits of various treatment methods.

## 7. Conclusion

AO is an extremely valuable tool in the study of the human visual system. Through bypassing the limitations of the optics of the eye, AO has enabled scientists to visualize single retinal cells *in vivo* and to probe the limits of human visual performance. Today, the field has moved on from technology development (although challenges still remain) to that of answering fundamental questions on retinal disease development and progression, human visual perception and aiding in the development of a range of new refractive technologies.

## 8. Acknowledgements

This work was supported in part by grant EY020901 from the National Institute of Health, Bethesda, MD, USA.

## 9. References

American National Standard Institute for the Safe Use of Lasers (ANSI). In Standard, A. N. (Ed.), (Vol. ANSI Z136.1 -- 2007): Laser Institute of America.

American National Standard Institute for the Safe Use of Lasers (ANSI). Ophthalmics Methods For Reporting Optical Aberrations Of Eyes. In (ANSI), A. N. S. I. (Ed.), (Vol. Z80.28-2010 ).

Artal, P., Chen, L., Fernandez, E. J., Singer, B., Manzanera, S. & Williams, D. R. (2004). Neural compensation for the eye's optical aberrations. *J Vis, 4*, 281-287.

Babcock, H. W. (1953). The possibility of compensating astronomical seeing. *Publ Astron Soc Pac, 65*, 229.

Bartsch, D. U., Zhu, L., Sun, P. C., Fainman, S. & Freeman, W. R. (2002). Retinal imaging with a low-cost micromachined membrane deformable mirror. *J Biomed Opt, 7*, 451-456.

Benito, A., Redondo, M. & Artal, P. (2009). Laser in situ keratomileusis disrupts the aberration compensation mechanism of the human eye. *Am J Ophthalmol, 147*, 424-431.

Bessho, K., Bartsch, D. U., Gomez, L., Cheng, L., Koh, H. J. & Freeman, W. R. (2009). Ocular wavefront aberrations in patients with macular diseases. *Retina, 29*, 1356-1363.

Burns, S. A., Wu, S., He, J. C. & Elsner, A. E. (1997). Variations in photoreceptor directionally across the central retina. *J Opt Soc Am A Opt Image Sci Vis, 14*, 2033-2040.

Campbell, F. W. & Green, D. G. (1965). Optical and retinal factors affecting visual resolution. *J Physiol, 181*, 576-593.

Carroll, J. (2008). Adaptive optics retinal imaging: applications for studying retinal degeneration. *Arch Ophthalmol, 126*, 857-858.

Carroll, J., Neitz, M., Hofer, H., Neitz, J. & Williams, D. R. (2004). Functional photoreceptor loss revealed with adaptive optics: an alternate cause of color blindness. *Proc Natl Acad Sci U S A, 101*, 8461-8466.

Carroll, J., Rossi, E. A., Porter, J., Neitz, J., Roorda, A., Williams, D. & Neitz, J. (2010). Deletion of the X-linked opsin gene array locus control region (LCR) results in disruption of the cone mosaic. *Vision Res, 50*, 1989–1899.

Chen, D. C., Jones, S. M., Silva, D. A. & Olivier, S. S. (2007a). High-resolution adaptive optics scanning laser ophthalmoscope with dual deformable mirrors. *J Opt Soc Am A Opt Image Sci Vis, 24*, 1305-1312.

Chen, L., Artal, P., Gutierrez, D. & Williams, D. R. (2007b). Neural compensation for the best aberration correction. *J Vis, 7*, 9 1-9.

Chen, L., Kruger, P. B., Hofer, H., Singer, B. & Williams, D. R. (2006). Accommodation with higher-order monochromatic aberrations corrected with adaptive optics. *J Opt Soc Am A Opt Image Sci Vis, 23*, 1-8.

Chen, Y., Ratnam, K., Sundquist, S. M., Lujan, B., Ayyagari, R., Gudiseva, V. H., Roorda, A. & Duncan, J. L. (2011). Cone photoreceptor abnormalities correlate with vision loss in patients with Stargardt disease. *Invest Ophthalmol Vis Sci, 52*, 3281-3292.

Chin, S. S., Hampson, K. M. & Mallen, E. A. (2009a). Effect of correction of ocular aberration dynamics on the accommodation response to a sinusoidally moving stimulus. *Opt Lett, 34*, 3274-3276.

Chin, S. S., Hampson, K. M. & Mallen, E. A. (2009b). Role of ocular aberrations in dynamic accommodation control. *Clin Exp Optom, 92*, 227-237.

Choi, S. S., Doble, N., Hardy, J. L., Jones, S. M., Keltner, J. L., Olivier, S. S. & Werner, J. S. (2006). In vivo imaging of the photoreceptor mosaic in retinal dystrophies and correlations with visual function. *Invest Ophthalmol Vis Sci, 47*, 2080-2092.

Choi, S. S., Enoch, J. M. & Kono, M. (2004). Evidence for transient forces/strains at the optic nerve head in myopia: repeated measurements of the Stiles-Crawford effect of the first kind (SCE-I) over time. *Ophthalmic Physiol Opt, 24*, 194-206.

Choi, S. S., Zawadzki, R. J., Keltner, J. L. & Werner, J. S. (2008). Changes in cellular structures revealed by ultra-high resolution retinal imaging in optic neuropathies. *Invest Ophthalmol Vis Sci, 49*, 2103-2119.

Choi, S. S., Zawadzki, R. J., Lim, M. C., Brandt, J. D., Keltner, J. L., Doble, N. & Werner, J. S. (2011). Evidence of outer retinal changes in glaucoma patients as revealed by ultrahigh-resolution in vivo retinal imaging. *Br J Ophthalmol, 95*, 131-141.

Chui, T. Y., Song, H. & Burns, S. A. (2008a). Adaptive-optics imaging of human cone photoreceptor distribution. *J Opt Soc Am A Opt Image Sci Vis, 25*, 3021-3029.

Chui, T. Y., Song, H. & Burns, S. A. (2008b). Individual variations in human cone photoreceptor packing density: variations with refractive error. *Invest Ophthalmol Vis Sci, 49*, 4679-4687.

Cooper, J., Citek, K. & Feldman, J. M. (2011). Comparison of refractive error measurements in adults with Z-View aberrometer, Humphrey autorefractor, and subjective refraction. *Optometry, 82*, 231-240.

Curcio, C. A. & Allen, K. A. (1990). Topography of ganglion cells in human retina. *J Comp Neurol, 300*, 5-25.

Curcio, C. A., Sloan, K. R., Kalina, R. E. & Hendrickson, A. E. (1990). Human photoreceptor topography. *J Comp Neurol, 292*, 497-523.

de Gracia, P., Dorronsoro, C., Marin, G., Hernandez, M. & Marcos, S. (2011). Visual acuity under combined astigmatism and coma: optical and neural adaptation effects. *J Vis, 11*.

Delori, F. C., Webb, R. H. & Sliney, D. H. (2007). Maximum permissible exposures for ocular safety (ANSI 2000), with emphasis on ophthalmic devices. *J Opt Soc Am A Opt Image Sci Vis, 24*, 1250-1265.

Diaz-Santana, L., Torti, C., Munro, I., Gasson, P. & Dainty, C. (2003). Benefit of higher closed-loop bandwidths in ocular adaptive optics. *Opt Express, 11*, 2597-2605.

Do, M. T. & Yau, K. W. (2010). Intrinsically photosensitive retinal ganglion cells. *Physiol Rev, 90*, 1547-1581.

Doble, N., Choi, S. S., Codona, J. L., Christou, J., Enoch, J. M. & Williams, D. R. (2011). In vivo imaging of the human rod photoreceptor mosaic. *Opt Lett, 36*, 31-33.

Doble, N., Miller, D. T., Yoon, G. & Williams, D. R. (2007). Requirements for discrete actuator and segmented wavefront correctors for aberration compensation in two large populations of human eyes. *Appl Opt, 46*, 4501-4514.

Doble, N., Yoon, G., Chen, L., Bierden, P., Singer, B., Olivier, S. & Williams, D. R. (2002). Use of a microelectromechanical mirror for adaptive optics in the human eye. *Opt Lett, 27*, 1537-1539.

Dreher, A. W., Bille, J. F. & Weinreb, R. N. (1989). Active optical depth resolution improvement of the laser tomographic scanner. *Appl Opt, 28*, 804-808.

Dubra A, Sulai Y, Norris JL, Cooper RF, Dubis AM, Williams DR, Carroll J. (2011). Noninvasive imaging of the human rod photoreceptor mosaic using a confocal adaptive optics scanning ophthalmoscope. *Biomed Opt Express*,2(7):1864-1876.

Duncan, J. L., Zhang, Y., Gandhi, J., Nakanishi, C., Othman, M., Branham, K. E., Swaroop, A. & Roorda, A. (2007). High-resolution imaging with adaptive optics in patients with inherited retinal degeneration. *Invest Ophthalmol Vis Sci, 48*, 3283-3291.

Einighammer, J., Oltrup, T., Feudner, E., Bende, T. & Jean, B. (2009). Customized aspheric intraocular lenses calculated with real ray tracing. *J Cataract Refract Surg, 35*, 1984-1994.

Elliott, D. B. & Chapman, G. J. (2009). Adaptive gait changes due to spectacle magnification and dioptric blur in older people. *Invest Ophthalmol Vis Sci, 51*, 718-722.

Elliott, S. L., Hardy, J. L., Webster, M. A. & Werner, J. S. (2007). Aging and blur adaptation. *J Vis, 7*, 8.

Enoch, J. M. (1963). Optical properties of the retinal receptors. *Journal of the Optical Society of America A, 53*, 71-85.

Fercher, A. F., Hitzenberger, C. K., Drexler, W., Kamp, G. & Sattmann, H. (1993). In vivo optical coherence tomography. *Am J Ophthalmol, 116*, 113-114.

Ferguson, R. D., Zhong, Z., Hammer, D. X., Mujat, M., Patel, A. H., Deng, C., Zou, W. & Burns, S. A. (2010). Adaptive optics scanning laser ophthalmoscope with integrated wide-field retinal imaging and tracking. *J Opt Soc Am A Opt Image Sci Vis, 27*, A265-277.

Fernandez, E. J. & Artal, P. (2005). Study on the effects of monochromatic aberrations in the accommodation response by using adaptive optics. *J Opt Soc Am A Opt Image Sci Vis, 22*, 1732-1738.

Fernandez, E. J., Iglesias, I. & Artal, P. (2001). Closed-loop adaptive optics in the human eye. *Opt Lett, 26*, 746-748.

Fernandez, E. J., Vabre, L., Hermann, B., Unterhuber, A., Povazay, B. & Drexler, W. (2006). Adaptive optics with a magnetic deformable mirror: applications in the human eye. *Opt Express, 14*, 8900-8917.

Fernández, E. & Drexler, W. (2005). Influence of ocular chromatic aberration and pupil size on transverse resolution in ophthalmic adaptive optics optical coherence tomography. *Opt Express, 13*, 8184-8197.

Gambra, E., Sawides, L., Dorronsoro, C. & Marcos, S. (2009). Accommodative lag and fluctuations when optical aberrations are manipulated. *J Vis, 9*, 4 1-15.

Genead, M. A., Fishman, G. A., Rha, J., Dubis, A. M., Bonci, D. M., Dubra, A., Stone, E. M., Neitz, M. & Carroll, J. (2011). Photoreceptor Structure and Function in Patients with Congenital Achromatopsia. *Invest Ophthalmol Vis Sci*.

Georgeson, M. A. & Sullivan, G. D. (1975). Contrast constancy: deblurring in human vision by spatial frequency channels. *J Physiol, 252*, 627-656.

Glanc, M., Gendron, E., Lacombe, F., Lafaille, D., Le Gargasson, J. F. & Léna , P. (2004). Towards wide-field retinal imaging with adaptive optics. *Optics Comm, 230*, 225-238.

Gray, D. C., Wolfe, R., Gee, B. P., Scoles, D., Geng, Y., Masella, B. D., Dubra, A., Luque, S., Williams, D. R. & Merigan, W. H. (2008). In vivo imaging of the fine structure of rhodamine-labeled macaque retinal ganglion cells. *Invest Ophthalmol Vis Sci, 49*, 467-473.

Gruppetta, S., Koechlin, L., Lacombe, F. & Puget, P. (2005). Curvature sensor for the measurement of the static corneal topography and the dynamic tear film topography in the human eye. *Opt Lett, 30*, 2757-2759.

Hampson, K. M., Chin, S. S. & Mallen, E. A. (2010). Effect of temporal location of correction of monochromatic aberrations on the dynamic accommodation response. *Biomed Opt Express, 1*, 879-894.

Hampson, K. M., Paterson, C., Dainty, C. & Mallen, E. A. (2006). Adaptive optics system for investigation of the effect of the aberration dynamics of the human eye on steady-state accommodation control. *J Opt Soc Am A Opt Image Sci Vis, 23*, 1082-1088.

Hardy, J. W. (1998). *Adaptive Optics for Astronomical Telescopes.* Oxford, UK: Oxford University Press.

He, J. C., Burns, S. A. & Marcos, S. (2000). Monochromatic Aberrations in the Accommodated Human Eye. *Vision Res, 40*, 41-48.

Headington, K., Choi, S. S., Nickla, D. & Doble, N. (2011). Single Cell, In vivo Imaging of the Chick Retina with Adaptive Optics. *Current Eye Research*, 36:947-957.

Hermann, B., Fernandez, E. J., Unterhuber, A., Sattmann, H., Fercher, A. F., Drexler, W., Prieto, P. M. & Artal, P. (2004). Adaptive-optics ultrahigh-resolution optical coherence tomography. *Opt Lett, 29*, 2142-2144.

Hofer, H., Artal, P., Singer, B., Aragon, J. L. & Williams, D. R. (2001a). Dynamics of the eye's wave aberration. *J Opt Soc Am A Opt Image Sci Vis, 18*, 497-506.

Hofer, H., Chen, L., Yoon, G. Y., Singer, B., Yamauchi, Y. & Williams, D. R. (2001b). Improvement in retinal image quality with dynamic correction of the eye's aberrations. *Opt Express, 8*, 631-643.

Huang, D., Swanson, E. A., Lin, C. P., Schuman, J. S., Stinson, W. G., Chang, W., Hee, M. R., Flotte, T., Gregory, K., Puliafito, C. A. & et al. (1991). Optical coherence tomography. *Science, 254*, 1178-1181.

Iftimia, N. V., Hammer, D. X., Bigelow, C. E., Ustun, T., de Boer, J. F. & Ferguson, R. D. (2006). Hybrid retinal imager using line-scanning laser ophthalmoscopy and spectral domain optical coherence tomography. *Opt Express, 14*, 12909-12914.

Iglesias, I., Ragazzoni, R., Julien, Y. & Artal, P. (2002). Extended source pyramid wave-front sensor for the human eye. *Opt Express, 10*, 419-428.

Joeres, S., Jones, S. M., Chen, D. C., Silva, D., Olivier, S., Fawzi, A., Castellarin, A. & Sadda, S. R. (2008). Retinal imaging with adaptive optics scanning laser ophthalmoscopy in unexplained central ring scotoma. *Arch Ophthalmol, 126*, 543-547.

Jonas, J. B., Schneider, U. & Naumann, G. O. H. (1992). Count and density of human retinal photoreceptors. *Graefe's Archive of Clinical and Experimental Ophthalmology, 230*, 505.

Jonnal, R. S., Besecker, J. R., Derby, J. C., Kocaoglu, O. P., Cense, B., Gao, W., Wang, Q. & Miller, D. T. (2010). Imaging outer segment renewal in living human cone photoreceptors. *Opt Express, 18*, 5257-5270.

Jonnal, R. S., Rha, J., Zhang, Y., Cense, B., Gao, W. & Miller, D. T. (2007). In vivo functional imaging of human cone photoreceptors. *Opt Express, 15*, 16141-16160.

Kanis, M. J. & van Norren, D. (2008). Delayed recovery of the optical Stiles-Crawford effect in a case of central serous chorioretinopathy. *British Journal of Ophthalmology, 92*, 292-292.

Katsoulos, C., Karageorgiadis, L., Vasileiou, N., Mousafeiropoulos , T. & Asimellis, G. (2009). Customized hydrogel contact lenses for keratoconus incorporating correction for vertical coma aberration. *Ophthalmic Physiol Opt, 29*, 321-329.

Kaufman, P. L. & Alm, A. (2002). *Adler's Physiology of the Eye* (10 ed.): Elsevier Health Sciences.

Kim, A. & Chuck, R. S. (2008). Wavefront-guided customized corneal ablation. *Curr Opin Ophthalmol, 19*, 314-320.

Kitaguchi, Y., Kusaka, S., Yamaguchi, T., Mihashi, T. & Fujikado, T. (2011). Detection of photoreceptor disruption by adaptive optics fundus imaging and Fourier-domain optical coherence tomography in eyes with occult macular dystrophy. *Clin Ophthalmol, 5*, 345-351.

Klaproth, O. K., Titke, C., Baumeister, M. & Kohnen, T. (2011). [Accommodative intraocular lenses - principles of clinical evaluation and current results]. *Klin Monbl Augenheilkd, 228*, 666-675.

Krueger, R. R. & Kanellopoulos, A. J. (2010). Stability of simultaneous topography-guided photorefractive keratectomy and riboflavin/UVA cross-linking for progressive keratoconus: case reports. *J Refract Surg, 26*, S827-832.

Kruger, P. B., Mathews, S., Aggarwala, K. R. & Sanchez, N. (1993). Chromatic aberration and ocular focus: Fincham revisited. *Vision Res, 33*, 1397-1411.

Larichev, A. V., Ivanov, P. V., Iroshnikov, N. G., Shmalhauzen , V. I. & Otten, L. J. (2002). Adaptive system for eye-fundus imaging. *Quantum Electronics, 32*, 902-908.

Li, F. H., Mukohzaba, N., Yoshida, N., Igasaki, Y., Toyoda, H., Inoue, T., Kobayashi, Y. & Hara, T. (1998). Phase modulation characteristics analysis of optically-addressed parallel-aligned nematic liquid crystal phase-only spatial light modulator combined with a liquid crystal display. *Opt Review, 5*, 174-178.

Li, K. Y., Tiruveedhula, P. & Roorda, A. (2010). Intersubject variability of foveal cone photoreceptor density in relation to eye length. *Invest Ophthalmol Vis Sci, 51*, 6858-6867.

Liang, C. & Williams, D. R. (1997). Aberrations and retinal image quality of the normal human eye. *J Opt Soc Am A Opt Image Sci Vis, 14*, 2873-2883.

Liang, J., Grimm, B., Goelz, S. & Bille, J. F. (1994). Objective measurement of wave aberrations of the human eye with the use of a Hartmann-Shack wave-front sensor. *J Opt Soc Am A Opt Image Sci Vis, 11*, 1949-1957.

Liang, J., Williams, D. R. & Miller, D. T. (1997). Supernormal vision and high-resolution retinal imaging through adaptive optics. *J Opt Soc Am A Opt Image Sci Vis, 14*, 2884-2892.

Lopez-Gil, N., Rucker, F. J., Stark, L. R., Badar, M., Borgovan, T., Burke, S. & Kruger, P. B. (2007). Effect of third-order aberrations on dynamic accommodation. *Vision Res, 47*, 755-765.

Makous, W., Carroll, J., Wolfing, J. I., Lin, J., Christie, N. & Williams, D. R. (2006). Retinal microscotomas revealed with adaptive-optics microflashes. *Invest Ophthalmol Vis Sci, 47*, 4160-4167.

Marmor, M. F., Choi, S. S., Zawadzki, R. J. & Werner, J. S. (2008). Visual insignificance of the foveal pit: reassessment of foveal hypoplasia as fovea plana. *Arch Ophthalmol, 126*, 907-913.

Martin, J. A. & Roorda, A. (2005). Direct and noninvasive assessment of parafoveal capillary leukocyte velocity. *Ophthalmology, 112*, 2219-2224.

McAllister, J. T., Dubis, A. M., Tait, D. M., Ostler, S., Rha, J., Stepien, K. E., Summers, C. G. & Carroll, J. (2010). Arrested development: high-resolution imaging of foveal morphology in albinism. *Vision Res, 50*, 810-817.

Merino, D., Dainty, C., Bradu, A. & Podoleanu, A. G. (2006). Adaptive optics enhanced simultaneous en-face optical coherence tomography and scanning laser ophthalmoscopy. *Opt Express, 14*, 3345-3353.

Merino, D., Duncan, J. L., Tiruveedhula, P. & Roorda, A. (2011). Observation of cone and rod photoreceptors in normal subjects and patients using a new generation adaptive optics scanning laser ophthalmoscope. *Biomed Opt Express, 2*, 2189-2201.

Miller, D. T., Kocaoglu, O. P., Wang, Q. & Lee, S. (2011). Adaptive optics and the eye (super resolution OCT). *Eye (Lond), 25*, 321-330.

Miller, D. T., Qu, J., Jonnal, R. S. & Thorn, K. (2003). Coherence Gating and Adaptive Optics in the Eye. *Proc. SPIE* 65-72.

Miller, D. T., Williams, D. R. & Morris, G. M. (1996). Images of cone photoreceptors in the living human eye. *Vision Res, 36*, 1067-1079.

Mujat, M., Ferguson, R. D., Patel, A. H., Iftimia, N., Lue, N. & Hammer, D. X. (2010). High resolution multimodal clinical ophthalmic imaging system. *Opt Express, 18*, 11607-11621.

Netter, F. H. (2006). *Netter's Atlas of Human Anatomy.* (4 ed.): Saunders-Elsevier.

Neuroscience Online. In Byrne, J. H. (Ed.): The University of Texas Health Science Center at Houston (UTHealth). 1997.

Noll, R. J. (1976). Zernike polynomials and atmospheric turbulence. *J Opt Soc Am A Opt Image Sci Vis, 66*, 207–211.

Pallikaris, A., Williams, D. R. & Hofer, H. (2003). The reflectance of single cones in the living human eye. *Invest Ophthalmol Vis Sci, 44*, 4580-4592.

Porter, J., Guirao, A., Cox, I. G. & Williams, D. R. (2001). Monochromatic aberrations of the human eye in a large population. *J Opt Soc Am A Opt Image Sci Vis, 18*, 1793-1803.

Porter, J., Queener, H., Lin, J., Thorn, K. E. & Awwal, A. (2006). *Adaptive Optics for Vision Science.* Hoboken, NJ Wiley-Interscience.

Prieto, P., Fernandez, E., Manzanera, S. & Artal, P. (2004). Adaptive optics with a programmable phase modulator: applications in the human eye. *Opt Express, 12*, 4059-4071.

Putnam, N. M., Hammer, D. X., Zhang, Y., Merino, D. & Roorda, A. (2010). Modeling the foveal cone mosaic imaged with adaptive optics scanning laser ophthalmoscopy. *Opt Express, 18*, 24902-24916.

Putnam, N. M., Hofer, H. J., Doble, N., Chen, L., Carroll, J. & Williams, D. R. (2005). The locus of fixation and the foveal cone mosaic. *J Vis, 5*, 632-639.

Putnam, N. M., Tiruveedhula, P. & Roorda, A. (2011). Characterization Of The Preferred Retinal Locus Of Fixation And The Locus Of Perceived Fixation In Relation To The Photoreceptor Mosaic *Association for Research and Vision in Ophthalmology*. Fort Lauderdale, Florida.

Ragazzoni, R. (1996). Pupil plane wavefront sensing with an oscillating prism. *J of Mod. Opt, 43*, 289-293.

Rha, J., Dubis, A. M., Wagner-Schuman, M., Tait, D. M., Godara, P., Schroeder, B., Stepien, K. & Carroll, J. (2010). Spectral domain optical coherence tomography and adaptive optics: imaging photoreceptor layer morphology to interpret preclinical phenotypes. *Adv Exp Med Biol, 664*, 309-316.

Rha, J., Jonnal, R. S., Thorn, K. E., Qu, J., Zhang, Y. & Miller, D. T. (2006). Adaptive optics flood-illumination camera for high speed retinal imaging. *Opt Express, 14*, 4552-4569.

Rocha, K. M., Vabre, L., Chateau, N. & Krueger, R. R. (2010). Enhanced visual acuity and image perception following correction of highly aberrated eyes using an adaptive optics visual simulator. *J Refract Surg, 26*, 52-56.

Roddier, F. (1988). Curvature sensing and compensation: a new concept in adaptive optics. *Appl Opt, 27*, 1223.

Roorda, A. (2011). Adaptive optics for studying visual function: a comprehensive review. *J Vis, 11*.

Roorda, A., Romero-Borja, F., Donnelly Iii, W., Queener, H., Hebert, T. & Campbell, M. (2002). Adaptive optics scanning laser ophthalmoscopy. *Opt Express, 10*, 405-412.

Roorda, A. & Williams, D. R. (1999). The arrangement of the three cone classes in the living human eye. *Nature, 397*, 520-522.

Roorda, A. & Williams, D. R. (2002). Optical fiber properties of individual human cones. *J Vis, 2*, 404-412.

Roorda, A., Zhang, Y. & Duncan, J. L. (2007). High-resolution in vivo imaging of the RPE mosaic in eyes with retinal disease. *Invest Ophthalmol Vis Sci, 48*, 2297-2303.

Rossi, E. A. & Roorda, A. (2010a). Is visual resolution after adaptive optics correction susceptible to perceptual learning? *J Vis, 10*, 11.

Rossi, E. A. & Roorda, A. (2010b). The relationship between visual resolution and cone spacing in the human fovea. *Nat Neurosci, 13*, 156-157.

Rossi, E. A., Weiser, P., Tarrant, J. & Roorda, A. (2007 ). Visual performance in emmetropia and low myopia after correction of high-order aberrations. *J Vis, 7*, 14.

Sabesan, R., Ahmad, K. & Yoon, G. (2007). Correcting highly aberrated eyes using large-stroke adaptive optics. *J Refract Surg, 23*, 947-952.

Sabesan R, Yoon G. (2010). Neural compensation for long-term asymmetric optical blur to improve visual performance in keratoconic eyes. *Invest Ophthalmol Vis Sci*, 51(7):3835-3839.

Sawides, L., de Gracia, P., Dorronsoro, C., Webster, M. & Marcos, S. (2011). Adapting to blur produced by ocular high-order aberrations. *J Vis, 11*.

Sawides, L., Gambra, E., Pascual, D., Dorronsoro, C. & Marcos, S. (2010). Visual performance with real-life tasks under adaptive-optics ocular aberration correction. *J Vis, 10*, 19.

Shack, R. B. & Platt, B. C. (1971). Production and use of a lenticular Hartmann screen. *J Opt Soc Am A Opt Image Sci Vis, 61*, 656.

Sincich, L. C., Zhang, Y., Tiruveedhula, P., Horton, J. C. & Roorda, A. (2009). Resolving single cone inputs to visual receptive fields. *Nat Neurosci, 12*, 967-969.

Snell, R. S. & Lemp, M. A. (1998). *Clinical Anatomy of the Eye* (2 ed.). Oxford: Backwell Science.

Stepien, K. E., Han, D. P., Schell, J., Godara, P. & Carroll, J. (2009). Spectral-domain optical coherence tomography and adaptive optics may detect hydroxychloroquine retinal toxicity before symptomatic vision loss. *Trans Am Ophthalmol Soc, 107*, 28-33.

Stevenson, S., Kumar, G. & Roorda, A. (2007). Psychophysical and oculomotor reference points for visual direction measured with the adaptive optics scanning laser ophthalmoscope. *J Vis, 7*, 137.

Stiles, W. S. & Crawford, B. H. (1933). The luminous efficiency of rays entering the eye pupil at different points. *Proceedings of the Royal Society of London. Series B: Biological Sciences, 112*, 428-450.

Swanson, E. A., Izatt, J. A., Hee, M. R., Huang, D., Lin, C. P., Schuman, J. S., Puliafito, C. A. & Fujimoto, J. G. (1993). In vivo retinal imaging by optical coherence tomography. *Opt Lett, 18*, 1864-1866.

Talcott, K. E., Ratnam, K., Sundquist, S. M., Lucero, A. S., Lujan, B. J., Tao, W., Porco, T. C., Roorda, A. & Duncan, J. L. (2011). Longitudinal study of cone photoreceptors during retinal degeneration and in response to ciliary neurotrophic factor treatment. *Invest Ophthalmol Vis Sci, 52*, 2219-2226.

Tam, J., Martin, J. A. & Roorda, A. (2010). Noninvasive visualization and analysis of parafoveal capillaries in humans. *Invest Ophthalmol Vis Sci, 51*, 1691-1698.

Thibos, L. N. & Bradley, A. (1997). Use of liquid-crystal adaptive-optics to alter the refractive state of the eye. *Optom Vis Sci, 74*, 581-587.

Thibos, L. N., Hong, X., Bradley, A. & Cheng, X. (2002). Statistical variation of aberration structure and image quality in a normal population of healthy eyes. *J Opt Soc Am A Opt Image Sci Vis, 19*, 2329-2348.

Tuten, W. S., Tiruveedhula, P. & Roorda, A. (2011). Adaptive Optics Scanning Laser Ophthalmoscope-based Microperimetry, *Association for Research and Vision in Ophthalmology*. Fort Lauderdale, Florida.

Tyson, R. K. (2010). *Principles of Adaptive Optics.* (3rd Edition ed.). USA: CRC Press.

Vargas-Martin, F., Prieto, P. M. & Artal, P. (1998). Correction of the aberrations in the human eye with a liquid-crystal spatial light modulator: limits to performance. *J Opt Soc Am A Opt Image Sci Vis, 15*, 2552-2562.

Vera-Diaz, F. A., Woods, R. L. & Peli, E. (2010). Shape and individual variability of the blur adaptation curve. *Vision Res, 50*, 1452-1461.

Vohnsen, B. (2007). Photoreceptor waveguides and effective retinal image quality. *J Opt Soc Am A Opt Image Sci Vis, 24*, 597-607.

Wade, A. & Fitzke, F. (1998). A fast, robust pattern recognition asystem for low light level image registration and its application to retinal imaging. *Opt Express, 3*, 190-197.

Wang, Q., Kocaoglu, O. P., Cense, B., Bruestle, J., Jonnal, R. S., Gao, W. & Miller, D. T. (2011). Imaging retinal capillaries using ultrahigh-resolution optical coherence tomography and adaptive optics. *Invest Ophthalmol Vis Sci, 52*, 6292-6299.

Webb, R. H., Hughes, G. W. & Pomerantzeff, O. (1980). Flying spot TV ophthalmoscope. *Appl Opt, 19*, 2991-2997.

Webster, M. A., Georgeson, M. A. & Webster, S. M. (2002). Neural adjustments to image blur. *Nat Neurosci, 5*, 839-840.

Webvision: The Organization of the Retina and Visual System. In Kolb, H., Nelson, R., Fernandez, E. & Jones, B. (Eds.): WorldPress. 2011.

Werner, J. S., Elliott, S. L., Choi, S. S. & Doble, N. (2009). Spherical aberration yielding optimum visual performance: evaluation of intraocular lenses using adaptive optics simulation. *J Cataract Refract Surg, 35*, 1229-1233.

Westheimer, G. (1967). Dependence of the magnitude of the Stiles-Crawford effect on retinal location. *J Physiol, 192*, 309-315.

Westheimer, G. (2008). Directional sensitivity of the retina: 75 years of Stiles-Crawford effect. *Proc Biol Sci, 275*, 2777-2786.

Wolfing, J. I., Chung, M., Carroll, J., Roorda, A. & Williams, D. R. (2006). High-resolution retinal imaging of cone-rod dystrophy. *Ophthalmology, 113*, 1019 e1011.

Yeh, S. I. & Azar, D. T. (2004). The future of wavefront sensing and customization. *Ophthalmol Clin North Am, 17*, 247-260.

Yoon, G. Y. & Williams, D. R. (2002). Visual performance after correcting the monochromatic and chromatic aberrations of the eye. *J Opt Soc Am A Opt Image Sci Vis, 19*, 266-275.

Yoon, M. K., Roorda, A., Zhang, Y., Nakanishi, C., Wong, L. J., Zhang, Q., Gillum, L., Green, A. & Duncan, J. L. (2009). Adaptive optics scanning laser ophthalmoscopy images in a family with the mitochondrial DNA T8993C mutation. *Invest Ophthalmol Vis Sci, 50*, 1838-1847.

Zawadzki, R. J., Cense, B., Zhang, Y., Choi, S. S., Miller, D. T. & Werner, J. S. (2008). Ultrahigh-resolution optical coherence tomography with monochromatic and chromatic aberration correction. *Opt Express, 16*, 8126-8143.

Zawadzki, R. J., Jones, S. M., Pilli, S., Balderas-Mata, S., Kim, D. Y., Olivier, S. S. & Werner, J. S. (2011). Integrated adaptive optics optical coherence tomography and adaptive optics scanning laser ophthalmoscope system for simultaneous cellular resolution in vivo retinal imaging. *Biomed Opt Express, 2*, 1674-1686.

Zhang, Y., Rha, J., Jonnal, R. & Miller, D. (2005). Adaptive optics parallel spectral domain optical coherence tomography for imaging the living retina. *Opt Express, 13*, 4792-4811.

Zhong, Z., Song, H., Chui, T. Y., Petrig, B. L. & Burns, S. A. (2011). Noninvasive measurements and analysis of blood velocity profiles in human retinal vessels. *Invest Ophthalmol Vis Sci, 52*, 4151-4157.

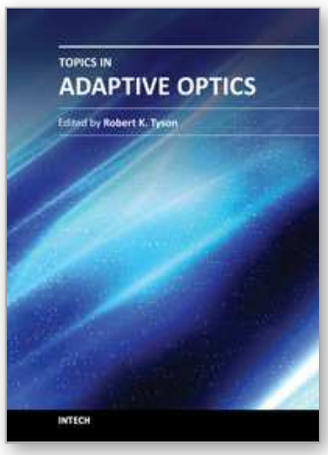


**Topics in Adaptive Optics**
Edited by Dr. Bob Tyson

ISBN 978-953-307-949-3
Hard cover, 254 pages
**Publisher** InTech
**Published online** 20, January, 2012
**Published in print edition** January, 2012

Advances in adaptive optics technology and applications move forward at a rapid pace. The basic idea of wavefront compensation in real-time has been around since the mid 1970s. The first widely used application of adaptive optics was for compensating atmospheric turbulence effects in astronomical imaging and laser beam propagation. While some topics have been researched and reported for years, even decades, new applications and advances in the supporting technologies occur almost daily. This book brings together 11 original chapters related to adaptive optics, written by an international group of invited authors. Topics include atmospheric turbulence characterization, astronomy with large telescopes, image post-processing, high power laser distortion compensation, adaptive optics and the human eye, wavefront sensors, and deformable mirrors.



**InTech Europe**
University Campus STeP Ri
Slavka Krautzeka 83/A
51000 Rijeka, Croatia
Phone: +385 (51) 770 447
Fax: +385 (51) 686 166
www.intechopen.com

**InTech China**
Unit 405, Office Block, Hotel Equatorial Shanghai
No.65, Yan An Road (West), Shanghai, 200040, China
中国上海市延安西路65号上海国际贵都大饭店办公楼405单元
Phone: +86-21-62489820
Fax: +86-21-62489821

IntechOpen